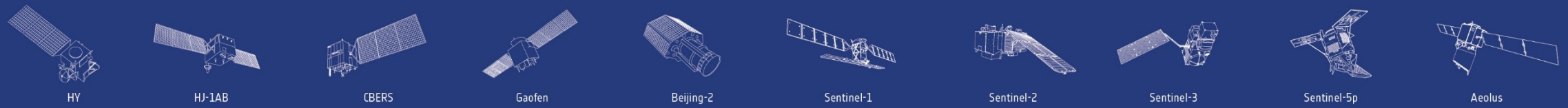


# 2023 DRAGON 5 SYMPOSIUM

## 3rd YEAR RESULTS REPORTING

## 11-15 SEPTEMBER 2023

**PROJECT ID. 58351**

# GLOBAL CLIMATE CHANGE, SEA LEVEL RISE, EXTREME EVENTS AND LOCAL GROUND SUBSIDENCE EFFECTS IN COASTAL AND RIVER DELTA REGIONS THROUGH NOVEL AND INTEGRATED REMOTE SENSING APPROACHES (GREENISH)

# Dragon 5 3rd Year Results Project

**13 SEPTEMBER 2023**

**ID. 58351**

**PROJECT TITLE: GREENISH**

**PRINCIPAL INVESTIGATORS: ANTONIO PEPE, QING ZHAO**

**AUTHORS: ANTONIO PEPE, FABIANA CALÒ, PIETRO MAESTRO, FRANCESCO FALABELLA, VIRGINIA ZAMPARELLI, QING ZHAO**

**PRESENTED BY: ANTONIO PEPE**

## Project Objectives

- Coastal zones are essential for the socio-economic well-being of many nations. Coastal regions are the location of large population centres, have multiple uses, needs and opportunities, and are particularly exposed to extreme events and climate change.

- The combined effects of sea level rise (SLR), storm surges, and extreme events can have numerous impacts to coastal, river delta, and inland water zones, including water management

- Global sea-level is rising, and tides are also changing worldwide and these risks are accompanied by increasing concerns about the growing urbanization of the world's low-lying coastal regions and related coastal hazards (e.g., flooding).

## Project Objectives

- The main goal of the project is the well-use of Earth Observation (EO) data to detect the long-term evolution of coastal, deltaic and lake-river systems.

- The results of some recent and on-going research activities will be presented.

- Over the third year of the project, we were mostly focused on the pubblication of papers and on putting in place of some AI methods for applications in coastal and urban zones.

# EO Data Delivery

Data access (list all missions and issues if any). NB. in the tables please insert cumulative figures (since July 2020) for no. of scenes of high bit rate data (e.g. S1 100 scenes). If data delivery is low bit rate by ftp, insert “ftp”

| ESA Third Party Missions | No. Scenes |
|---|---|
| 1. CSK | 10 |
| 2. | |
| 3. | |
| 4. | |
| 5. | |
| 6. | |
| Total: | |
| Issues: | |

| ESA /Copernicus Missions | No. Scenes |
|---|---|
| 1.SENTINEL-1A/B | 800 |
| 2. | |
| 3. | |
| 4. | |
| 5. | |
| 6. | |
| Total: | 800 |
| Issues: | |

| Chinese EO data | No. Scenes |
|---|---|
| 1. | |
| 2. | |
| 3. | |
| 4. | |
| 5. | |
| 6. | |
| Total: | |
| Issues: | |

# European Young scientists contributions in Dragon 5

| Name | Institution | Poster title | Contribution |
|---|---|---|---|
| Pietro Mastro | National Research Council of Italy, IREA-CNR | Risk Analysis in Coastal and Cultural Heritage Areas Using SAR and AI-Based Change Detection Methodologies: The Case Study of Venice Lagoon | The work investigates ground displacements and land changes occurred in Venice Lagoon in the recent years, with reference specifically to extreme flood events that occurred in November 2019. A joint multi-pass coherent/incoherent change detection strategy is proposed. The paper investigates the role of Change Detection and InSAR methods for the Retrieval and Tracking of Changes in Inundated/Fire-Prone Regions. |

*Dr. Mastro cannot participate to the D5 meeting but the poster and the e-poster are available

# Chinese Young scientists contributions in Dragon 5

| Name | Institution | Poster title | Contribution including period of research |
|---|---|---|---|
| Peng Chen, Qing Zhao | [1]Key Laboratory of Geographical Information Science, Ministry of Education, East China Normal University, Shanghai 200062, China; [2]School of Geographic Sciences, East China Normal University, Shanghai 200241, China ; [3]Key Laboratory of Spatial-Temporal Big Data Analysis and Application of Natural Resources in Megacities, Ministry of Natural Resources, Shanghai 200241, China | DSPA-Net: A deeply supervised pseudo-siamese attention-guided network for building change detection with intensity and coherence information of SAR images | We proposed a deeply supervised pseudo-siamese attention-guided network (DSPA-Net) for BCD, in which convolutional blocks have a strong ability in noise reduction owing to the large receptive fields, and the adopted pseudo-siamese structure does well in extracting intensity information and coherence information with the same network branch but different weights. Besides, different blocks were used to optimize the network model. |

# Chinese Young scientists contributions in Dragon 5

| Name | Institution | Poster title | Contribution including period of research |
|---|---|---|---|
| Lei Zhou, Qing Zhao | [1]Key Laboratory of Geographical Information Science, Ministry of Education, East China Normal University, Shanghai 200062, China; [2]School of Geographic Sciences, East China Normal University, Shanghai 200241, China ; [3]Key Laboratory of Spatial-Temporal Big Data Analysis and Application of Natural Resources in Megacities, Ministry of Natural Resources, Shanghai 200241, China | Information extraction and quantifying migration of saltmarsh vegetation in Chongming Dongtan Wetland by integrating multi-source remote sensing data and phenological characteristics during 2017-2022 | According to the particularity of the estuary wetland in Chongming Dongtan Wetland, different characteristic parameters are calculated, including vegetation index, water body index, spectral feature, radar feature, texture feature and time feature. Six multi-dimensional feature data sets containing different feature parameters have been formulated. We perform object-oriented multi-scale inheritance segmentation on six feature data sets, and use segmentation parameter optimization tool to select the optimal segmentation parameters. Combined with field investigation and visual interpretation of high-resolution remote sensing images, we build a classification system of Chongming Dongtan Wetland Saltmarsh Vegetation, which mainly includes three types of wetland saltmarsh vegetation: Phragmites australis, Spartina alterniflora and Scirpus mariqueter. This study also uses Sentinel-2, Sentinel-1 and Landsat8 fusion images based on Google Earth Engine(GEE) to construct a medium-resolution long-term median image dataset, to obtain the spatio-temporal distribution results of saltmarsh vegetation in Chongming Dongtan Wetland from 2017 to 2022 and the quantitative migration of saltmarsh vegetation. |

# Chinese Young scientists contributions in Dragon 5

| Name | Institution | Poster title | Contribution including period of research |
|---|---|---|---|
| Jingjing Wang, Qing Zhao | [1]Key Laboratory of Geographical Information Science, Ministry of Education, East China Normal University, Shanghai 200062, China; [2]School of Geographic Sciences, East China Normal University, Shanghai 200241, China ; [3]Key Laboratory of Spatial-Temporal Big Data Analysis and Application of Natural Resources in Megacities, Ministry of Natural Resources, Shanghai 200241, China | Construction and Application of Comprehensive Risk Assessment Model for Disaster-bearing Bodies in Mega-city Based on Multiple Natural Disaster Scenarios | We constructed a comprehensive risk assessment indicator system using three dimensions hazard, vulnerability, and exposure. The risk assessment model of disaster-bearing bodies was constructed by weighted calculation input indexes and realized automatic comprehensive risk assessment of the disaster-bearing bodies. The weights of input indexes are determined by summarizing historical disaster data and scored by experts. We use this model to evaluate the comprehensive risk level of the disaster-bearing bodies under multiple natural disaster scenarios and analyze the distribution of risk levels. The regional disaster reduction capacity of Shanghai and the comprehensive risk level of the disaster-bearing bodies were combined with a disaster matrix to determine which high-risk disaster-bearing bodies located in areas with low disaster reduction capacity. |

# Exchange Activities and Recruitment Plans

- Chinese researchers and students have been working remotely with CNR-IREA scientists in Italy
- A new visit to East China Normal University, Shanghai is planned by the end of this year to finalize present activities and plan those to be proposed within the forthcoming D6 programme.
- I have been selected to be part of the Chinese High-End Foreign Experts Recruitment Program that funds periods of exchange in China, seminars, on-line teaching and various other resources.
- Two Research Grants ("Assegno di Ricerca") for Young Scientists (< 35 years old), co-funded with ESA and CNR-IREA internal funds officially started on November 1, 2023.

The schedule of the GREENISH YS recruitment and training (Gaant Chart) is pictorially shown in Figure 1

| | ago-21 | | | | | | | | | | | lug-22 | ago-22 | | | nov-22 | | | | | | | lug-23 | | | ott-23 | | | | feb-24 | | | | | lug-24 |
|---|---|---|---|---|---|---|---|---|---|---|---|---|---|---|---|---|---|---|---|---|---|---|---|---|---|---|---|---|---|---|---|---|---|---|
| | 1 | 2 | 3 | 4 | 5 | 6 | 7 | 8 | 9 | 10 | 11 | 12 | 13 | 14 | 15 | 16 | 17 | 18 | 19 | 20 | 21 | 22 | 23 | 24 | 25 | 26 | 27 | 28 | 29 | 30 | 31 | 32 | 33 | 34 | 35 | 36 |
| Project Management | | | | | | | | | | | | | | | | | | | | | | | | | | | | | | | | | | | | |
| Post-Graduate Recruiting | | | | | | | | | | | | | | | | | | | | | | | | | | | | | | | | | | | | |
| Post-Graduate Training and Activities | | | | | | | | | | | | | | | | | | | | | | | | | | | | | | | | | | | | |
| Post-Doc Recruiting | | | | | | | | | | | | | | | | | | | | | | | | | | | | | | | | | | | | |
| Post-Doc Training and Activities | | | | | | | | | | | | | | | | | | | | | | | | | | | | | | | | | | | | |

T0

TO: D5 meeting in July 2021

Figure 1: Gaant Chart

# Innovative remote sensing methodologies and applications in coastal and marine environments

Qing Zhao[a,b,c], Antonio Pepe[d,e], Virginia Zamparelli[d], Pietro Mastro[d], Francesco Falabella[d,f], Saygin Abdikan[g], Caglar Bayik[h], Fusun Balik Sanli[i], Mustafa Ustuner[j], Nevin Betul Avşar[k], Jingjing Wang[a,b,c], Peng Chen[a,b,c], Zhengjie Li[a,b,c], Adam T. Devlin[l] and Fabiana Calò[d]

[a]Key Laboratory of Geographical Information Science, Ministry of Education, East China Normal University, Shanghai, China; [b]School of Geographic Sciences, East China Normal University, Shanghai, China; [c]Key Laboratory of Spatial-Temporal Big Data Analysis and Application of Natural Resources in Megacities, Ministry of Natural Resources, Shanghai, China; [d]Institute for Electromagnetic Sensing of the Environment (IREA), Italian National Research Council, Napoli, Italy; [e]School of Engineering, University of Basilicata, Potenza, Italy; [f]Institute of Methodologies for Environmental Analysis (IMAA), Italian National Research Council, Tito Scalo, Italy; [g]Department of Geomatics Engineering, Hacettepe University, Ankara, Turkey; [h]Department of Geomatics Engineering, Zonguldak Bulent Ecevit University, Zonguldak, Turkey; [i]Department of Geomatic Engineering, Yildiz Technical University, Istanbul, Turkey; [j]Department of Geomatic Engineering, Artvin Çoruh University, Artvin, Turkey; [k]Department of Geomatics Engineering, Izmir Katip Celebi University, İzmir, Turkey; [l]School of Ocean and Earth Science and Technology, University of Hawaii at Mānoa, Honolulu, HI, USA

**ABSTRACT**

Remote sensing (RS) technologies are extensively exploited by scientists and a vast audience of local authorities, urban managers, and city planners. Coastal regions, geohazard-prone areas, and highly populated cities represent natural laboratories to apply RS technologies and test new methods. Over the last decades, many efforts have been spent on improving Earth's surface monitoring, including intensifying Earth Observation (EO) operations by the major national space agencies. They oversee to plan and make operational constellations of satellite sensors providing the scientific community with extensive research and development opportunities in the geoscience field. For instance, within this framework, the European Space Agency (ESA) and the Ministry of Science and Technology of China (MOST) have sponsored, since the early 2000s, the DRAGON initiative jointly carried out by the European and Chinese RS scientific communities. This manuscript aims to provide a synthetic overview of some research activities and new methods recently designed and applied and trace the route for further developments. The main findings are related to i) the analysis of flood risk in China, ii) the potential of new methods for the estimation and removal of ground displacement biases in small-baseline oriented interferometric Synthetic Aperture Radar (SAR) methods, iii) the analysis of the inundation risk in low-lying regions using coherent and incoherent SAR methods; and iv) the use of SAR-based technologies for marine applications.

**ARTICLE HISTORY**
Received 30 January 2023
Accepted 31 July 2023

**KEYWORDS**
Disaster risk management; Remote Sensing (RS); Earth Observation (EO); Synthetic Aperture Radar (SAR); flooding; subsidence; coastal/marine environments

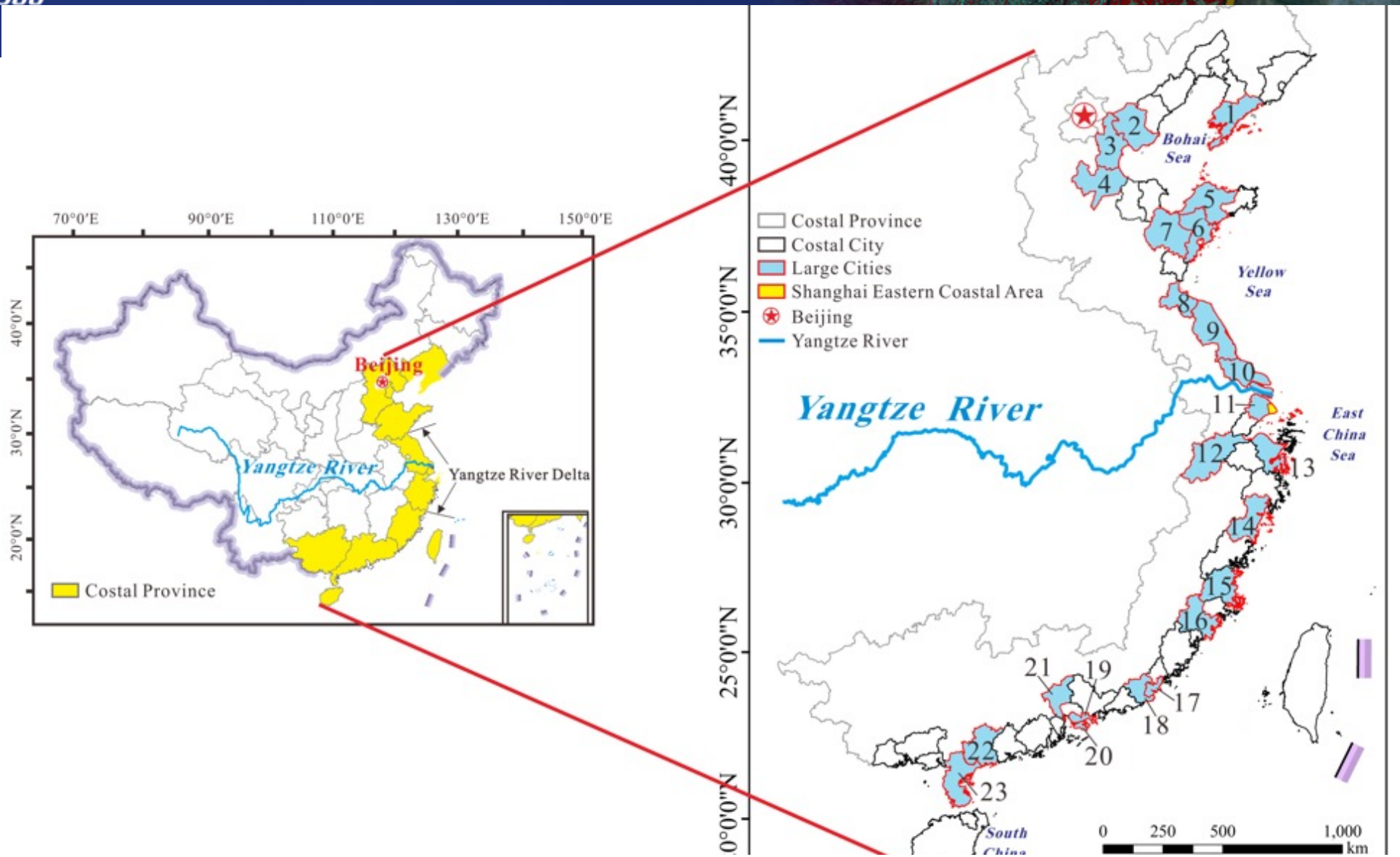
70°0'E
90°0'E
110°0'E
130°0'E
150°0'E
40°0'N
30°0'N
20°0'N
Beijing
Yangtze River
Yangtze River Delta
Costal Province
Costal Province
Costal City
Large Cities
Shanghai Eastern Coastal Area
Beijing
Yangtze River
Yangtze River
Bohai Sea
Yellow Sea
East China Sea
South China
1
2
3
4
5
6
7
8
9
10
11
12
13
14
15
16
17
18
19
20
21
22
23
40°0'0"N
35°0'0"N
30°0'0"N
25°0'0"N
0
250
500
1,000
km

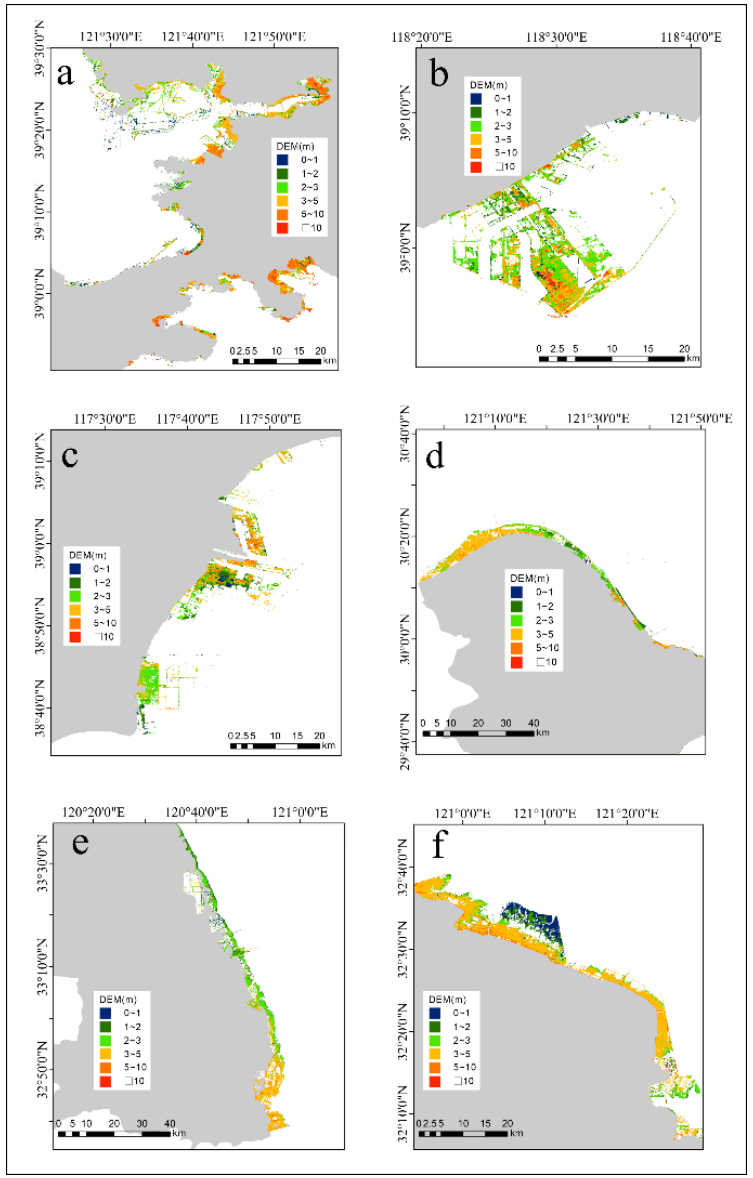


The terrain elevation changes of newly reclaimed land in selected coastal areas, i.e., (a) Dalian, (b) Tangshan, (c) Tianjin, (d) Ningbo, (e) Yancheng, (f) Nantong, obtained by comparing SRTM DEM (2000) and TanDEM-X (2015) (Tang et al. 2022).

*remote sensing*

MDPI

*Article*

## Changes of Chinese Coastal Regions Induced by Land Reclamation as Revealed through TanDEM-X DEM and InSAR Analyses

**Maochuan Tang [1,2,3], Qing Zhao [1,2,3,*], Antonio Pepe [4], Adam Thomas Devlin [5,6,7], Francesco Falabella [4,8,9], Chengfang Yao [1,2,3] and Zhengjie Li [1,2,3]**

1 Key Laboratory of Geographical Information Science, Ministry of Education, East China Normal University, Shanghai 200241, China; 51193901043@stu.ecnu.edu.cn (M.T.); 51203901043@stu.ecnu.edu.cn (C.Y.); 51203901076@stu.ecnu.edu.cn (Z.L.)
2 Institute of Eco-Chongming (I.E.C.), East China Normal University, Shanghai 202162, China
3 School of Geographic Sciences, East China Normal University, Shanghai 200241, China
4 Institute for Electromagnetic Sensing of the Environment (IREA), Italian National Research Council, 328, Diocleziano, 80124 Napoli, Italy; pepe.a@irea.cnr.it (A.P.); francesco.falabella@unibas.it (F.F.)
5 Key Laboratory of Poyang Lake Wetland and Watershed Research of Ministry of Education, Nanchang 330022, China; atdevlin@jxnu.edu.cn
6 School of Geography and Environment, Jiangxi Normal University, Nanchang 330022, China
7 Institute of Space and Earth Information Science, The Chinese University of Hong Kong, Shatin, Hong Kong, China
8 Institute of Methodologies for Environmental Analysis (IMAA), Italian National Research Council, Tito Scalo, 85050 Potenza, Italy
9 School of Engineering, University of Basilicata, 85100 Potenza, Italy
* Correspondence: qzhao@geo.ecnu.edu.cn; Tel.: +86-21-62224459

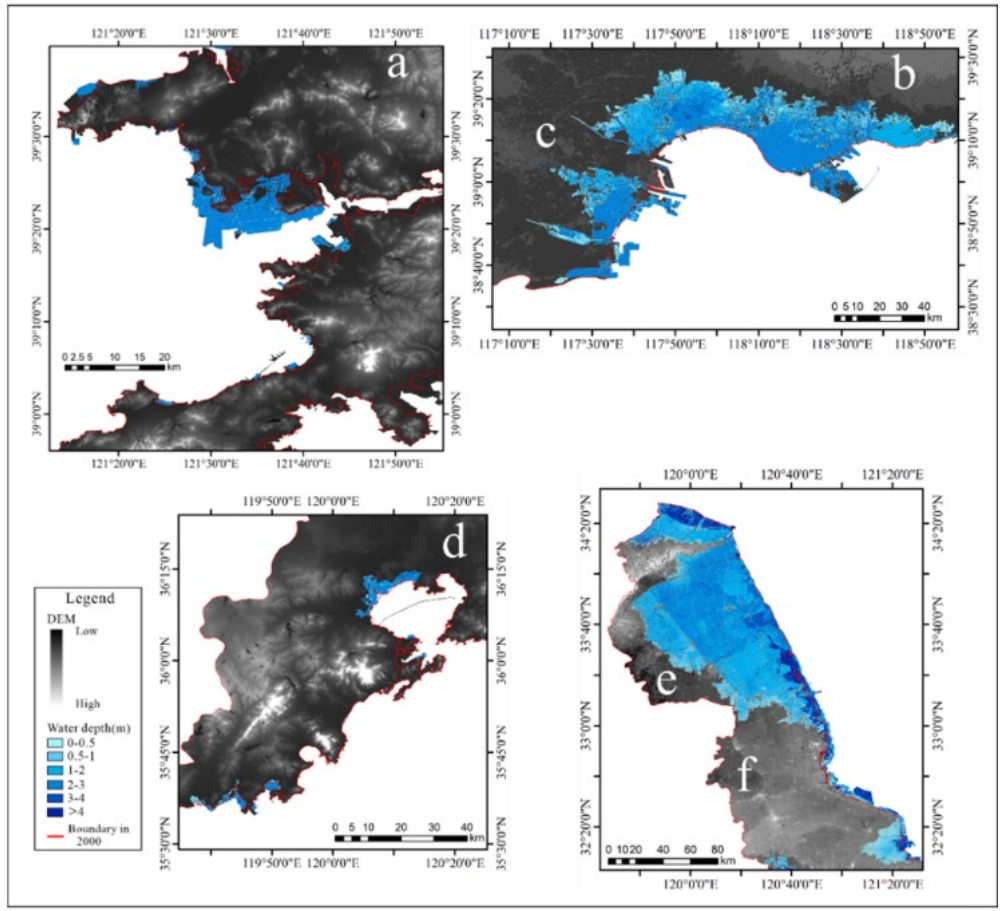


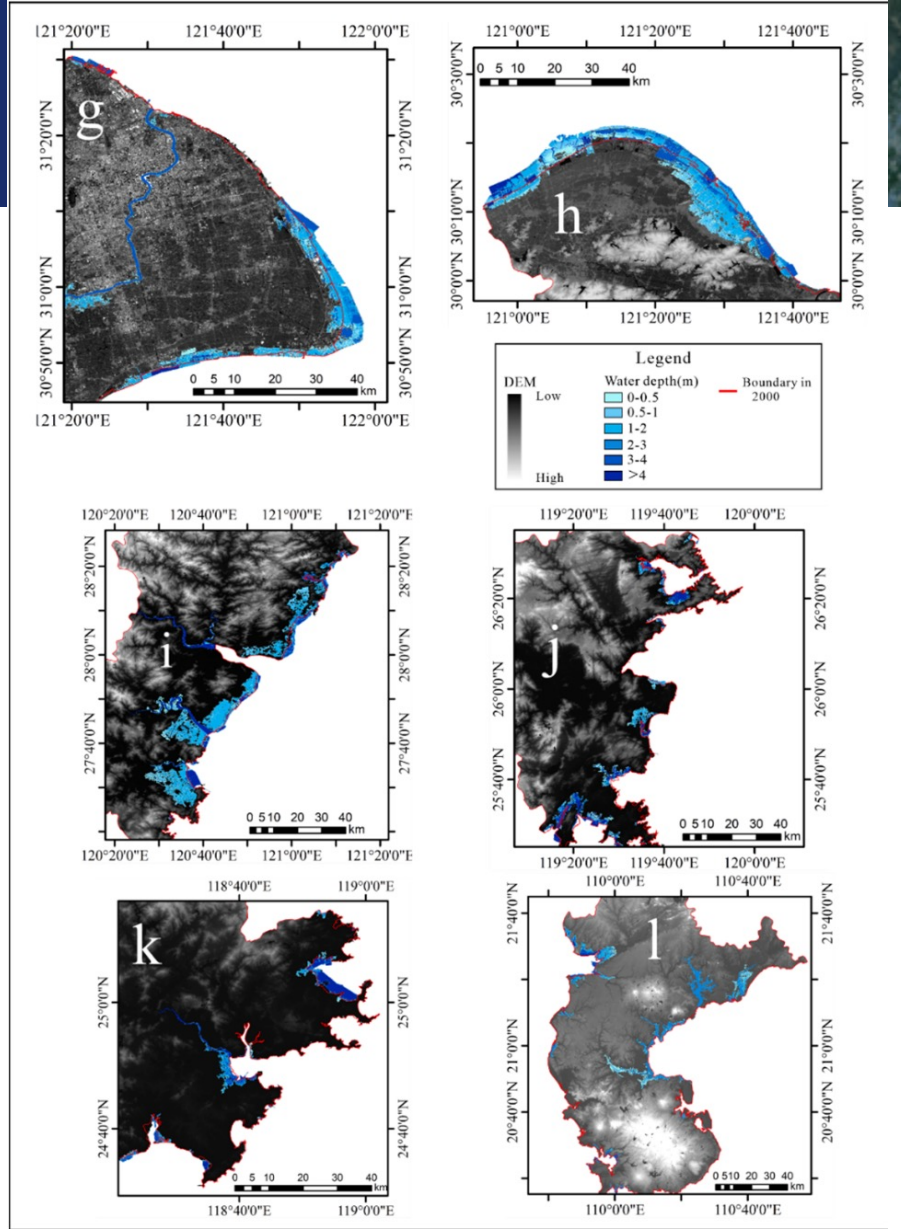


Inundation maps under a 100-year return period flood for: (a) Dalian; (b,c) Tangshan–Tianjin; (d) Qingdao; (e,f) Yancheng–Nantong; (g) Shanghai; (h) Ningbo; (i) Wenzhou; (j) Fuzhou; (k) Quanzhou; and (l) Zhanjiang.

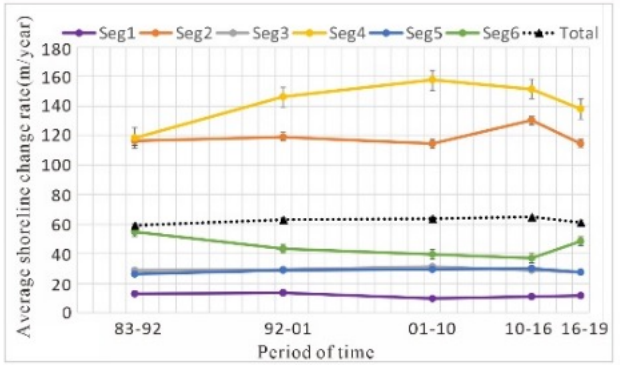


**Shoreline change rate(m/year) in different segments**

| Seg | Max | Min | Average |
|---|---|---|---|
| Seg1 | 127.9±21.7 | −39.6±6.6 | 11.8±5.5 |
| Seg2 | 615.0±1.5 | −2.4±0.5 | 118.9±21.3 |
| Seg3 | 203.8±31.0 | −19.1±7.6 | 29.4±7.5 |
| Seg4 | 560.7±44.4 | 0.0±0.0 | 141.3±26.3 |
| Seg5 | 508.9±59.2 | −321.5±70.8 | 28.7±8.7 |
| Seg6 | 472.4±115.0 | −4.5±2.4 | 44.8±10.5 |


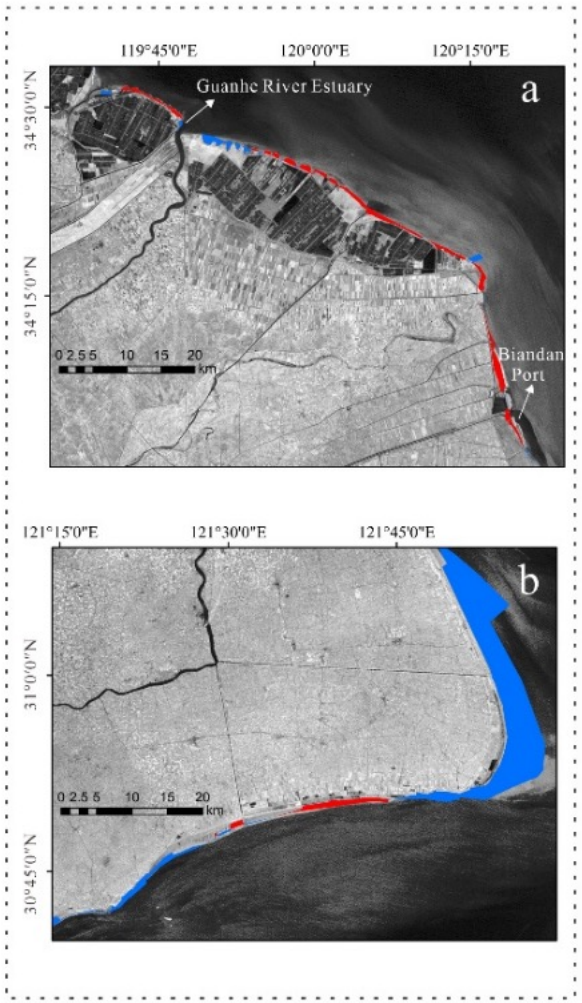


Area variation and rate of coastline change in the Yangtze Delta. The delta's shoreline was divided into six segments based on coastline change rates and geographical characteristics. The separation of segments 1 and 2 was due to the reclamation intensity. Segment 2 to segment 5 were divided by the Yangtze Estuary, the Qiantang River Estuary, and the Yongjiang River Estuary from north to south. Segment 6 consists of three islands administered by Shanghai. Sections (a,b) indicate locations where shoreline erosion has occurred

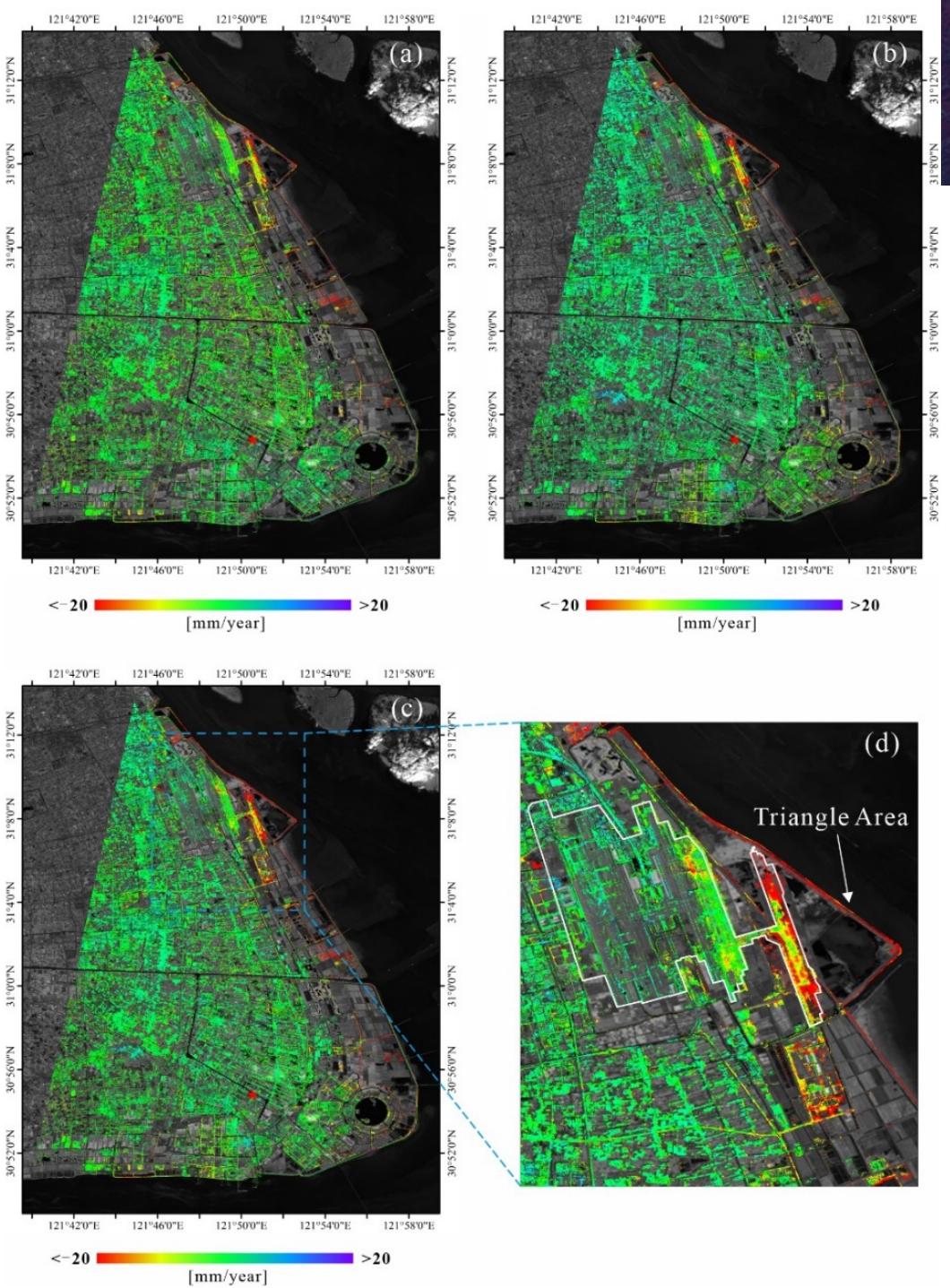


(a) Map of geocoded mean LOS deformation velocity calculated with the S-1A ground deformation time-series, from March 2018 to August 2021. (b) Map of geocoded mean LOS deformation velocity calculated with the CSK ground deformation time-series, from March 2018 to June 2021. (c) Map of geocoded mean deformation velocity in the Up–Down direction from 2018 to 2021 derives from two SAR datasets in the ascending and descending paths, respectively. The red star represents the location of the reference pixel. (d) Zoom of the area within the blue box shown in (c). The white polygon highlights Pudong Airport.

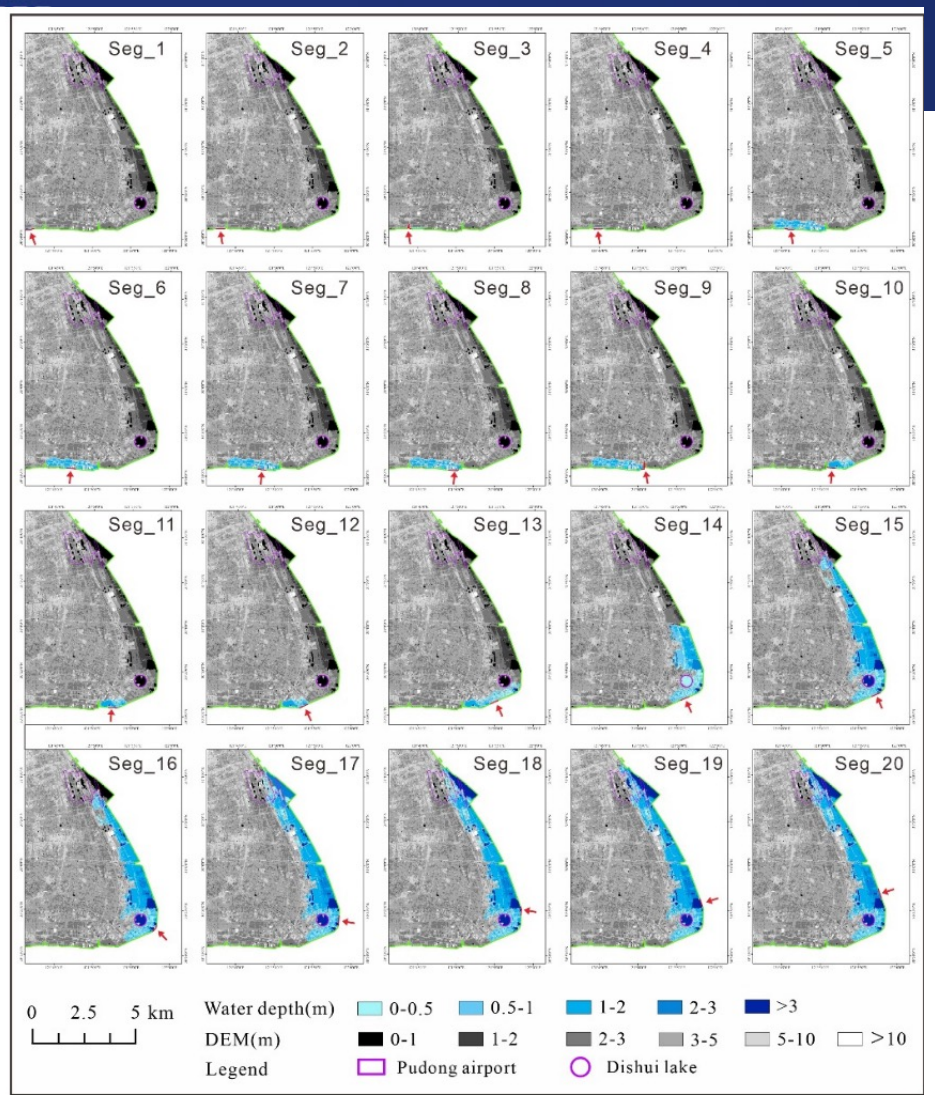


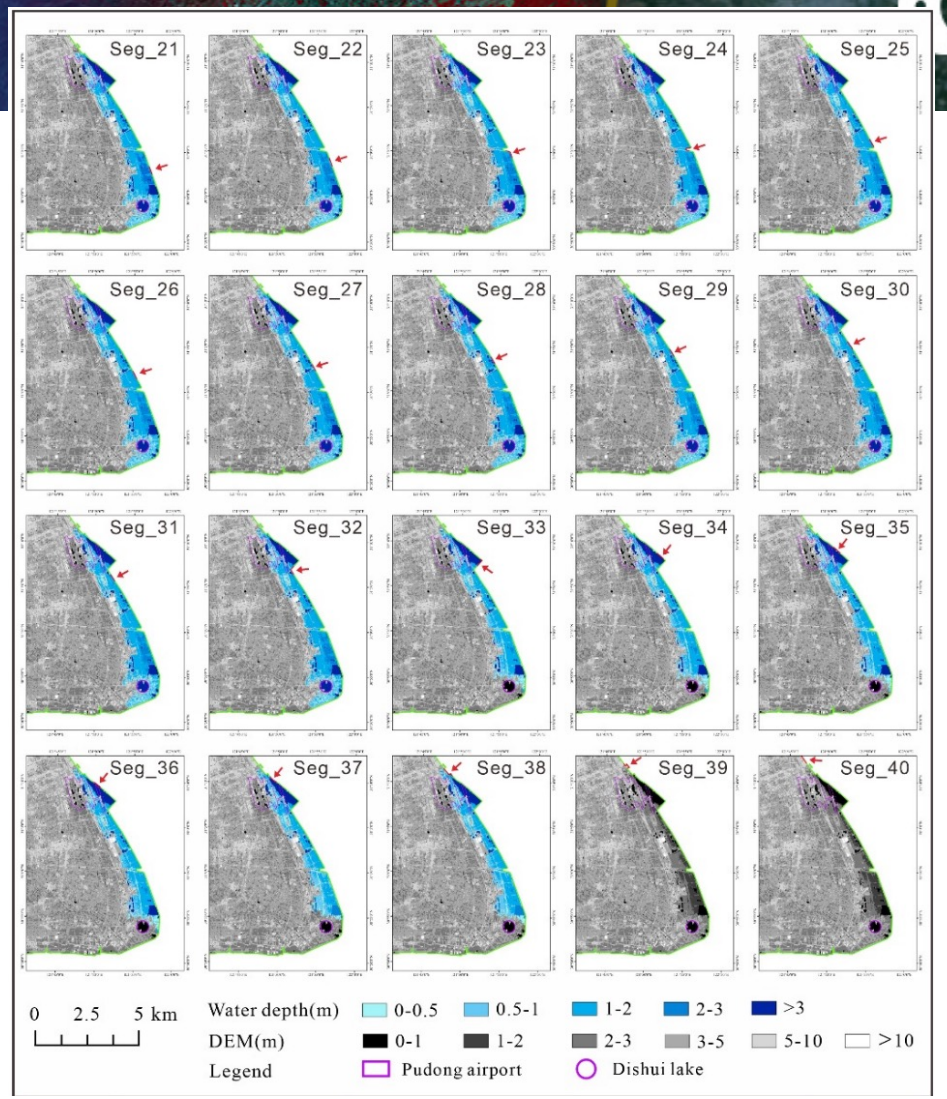


Simulated inundation scenarios for a 100-year return period flood in Shanghai. The section where each red arrow points is the location where the wave is assumed to overtop

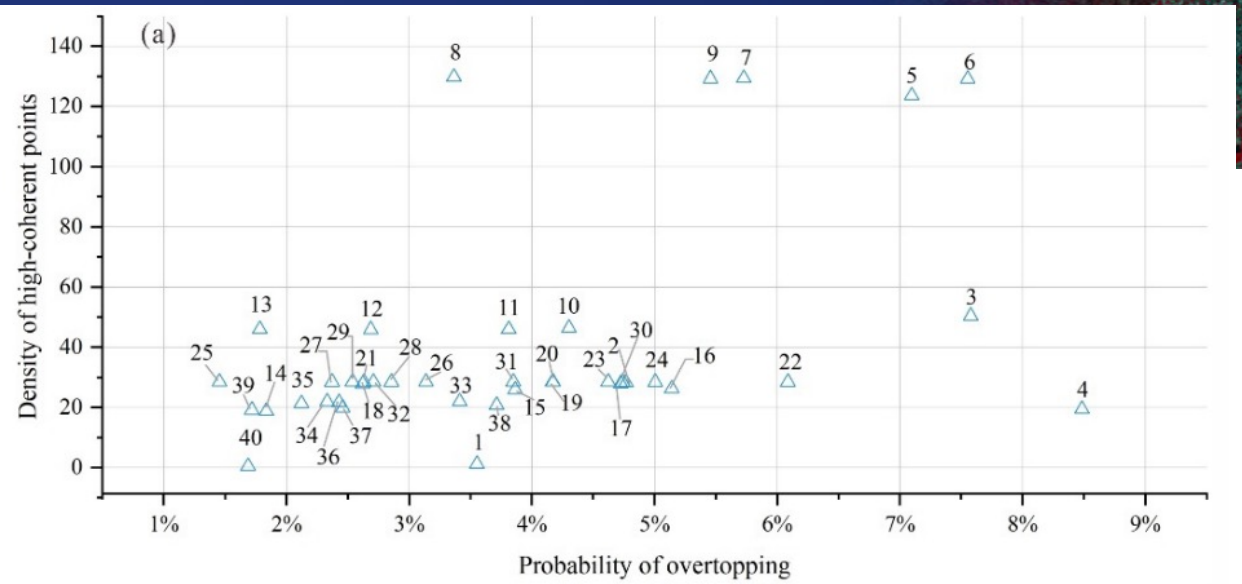


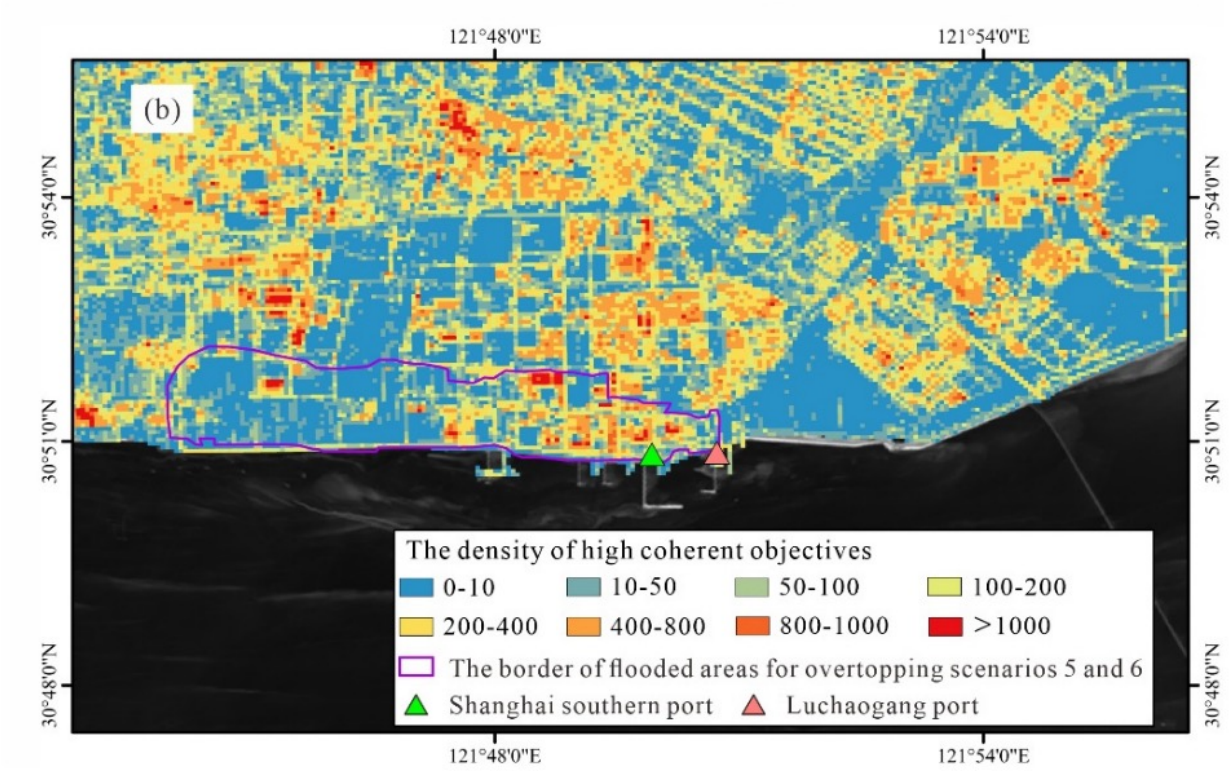


(a) The overtopping flood risk map for the selected 40 segments of the Shanghai seawalls. The X-axis shows the probability of overtopping, and Y-axis is the impact of a flood, measured as the density of high-coherent points affected by the flood. (b) Zoom-in view of southern Shanghai. The purple polygon shows the density of high-coherent objects within the flooded areas for overtopping scenarios 5 and 6. The coherent target density was calculated as the number of points in a 90 × 90 m grid.

IEEE TRANSACTIONS ON GEOSCIENCE AND REMOTE SENSING

# Phase Closure Inconsistencies of Multi-look SAR Interferogram Triplets

Francesco Falabella, *Graduate Student Member, IEEE*, and Antonio Pepe, *Senior Member, IEEE*

- The multi-look operation involves the average of the information relating to each family of scatterers in the single look (SLC) pixels.

- Recently, it has been observed that some inconsistencies in the InSAR products (i.e., ground deformation time-series and mean deformation velocity maps) may happen when sets of multi-look SAR interferograms with very short temporal baselines are processed.

- Such spurious signals lead to systematic biases that might lead to unreliable InSAR ground displacement products

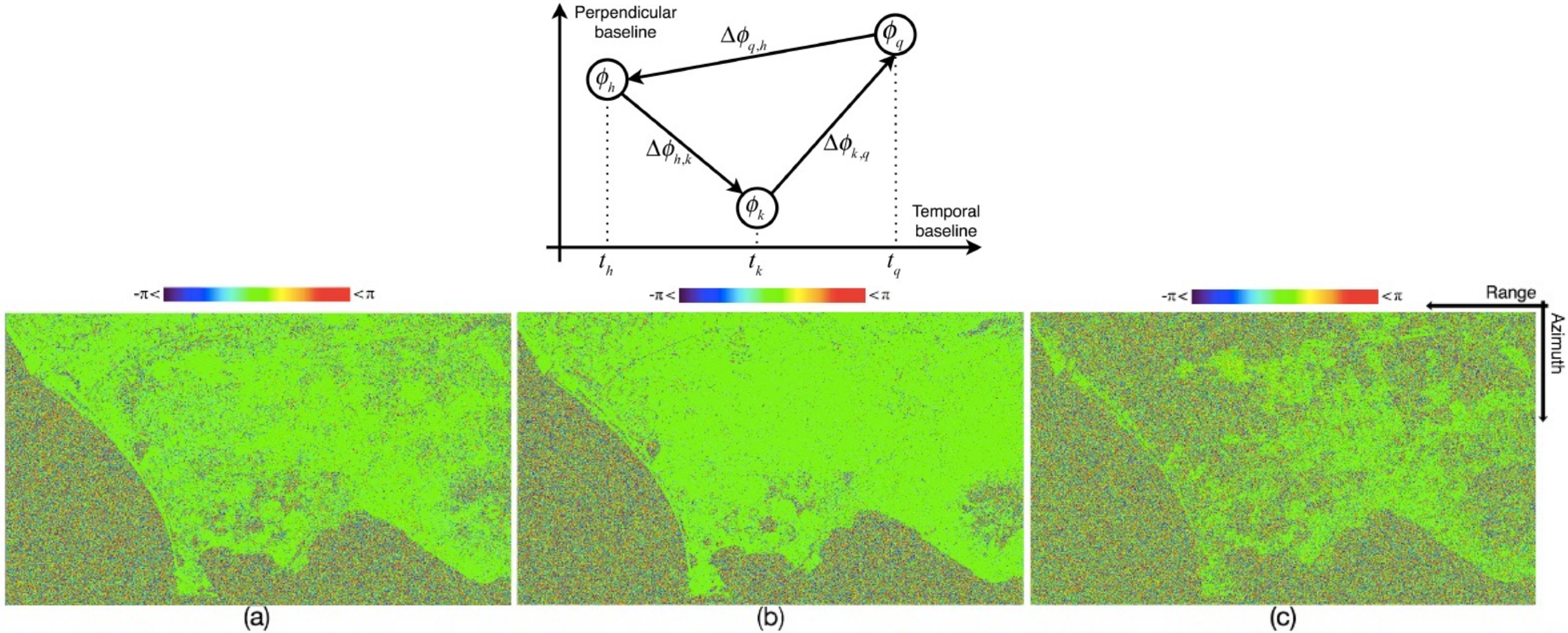


Fig. 6. COSMO-SkyMed phase triplets over the Gulf of Naples, Italy. a) Triplet's epochs: 2011-06-17, 2011-06-18, and 2011-06-21. Triplet's average absolute perpendicular baseline: 140 m. b) Triplet's time instants: 2010-02-14, 2010-02-22, and 2010-02-23. Triplet's average absolute perpendicular baseline: 113 m. c) Triplet's time instants: 2010-07-24, 2010-08-25, and 2010-10-12. Triplet's average absolute perpendicular baseline: 246 m.

Let us assume that the biased phases are time-invariant, i.e., the bias phenomena depends only on the temporal baseline values $\Delta t_{h,k}$, thus we model the InSAR biased phases with a second order expansion as follows:

$$\Delta\phi_{h,k}^{bias}\left(\Delta t_{h,k}\right)\cong\left[v+\Delta v\left(\Delta t_{h,k}\right)\right]\Delta t_{h,k} \tag{1}$$

where $v$ is a constant decay phase velocity factor and $\Delta v$ is a temporal-baseline-dependent phase velocity difference term. If we consider two generic interferometric SAR data pairs with temporal baselines $(\lambda-1)\delta$ and $\lambda\delta$, where $\delta$ is the repetition time of the considered SAR constellation (i.e., 6 days for Sentinel-1A/B sensors) and , Equation (1) particularizes as:

$$\Delta\phi^{bias}\left(\lambda\delta\right)\cong\left[v+\Delta v\left(\lambda\delta\right)\right]\lambda\delta \tag{2}$$

$$\Delta\phi^{bias}\left[\left(\lambda-1\right)\delta\right]\cong\left\{v+\Delta v\left[\left(\lambda-1\right)\delta\right]\right\}\left(\lambda-1\right)\delta \tag{3}$$

Equations (2) and (3) can properly be combined with each other, and the following iterative relation is found:

$$\Delta\phi^{bias}\left[\left(\lambda-1\right)\delta\right]\cong\frac{\lambda-1}{\lambda}\Delta\phi^{bias}\left(\lambda\delta\right)+\left\{\Delta v\left[\left(\lambda-1\right)\delta\right]-\Delta v\left(\lambda\delta\right)\right\}\left(\lambda-1\right)\delta \tag{4}$$

# Dragon 5 Mid-term Results Reporting

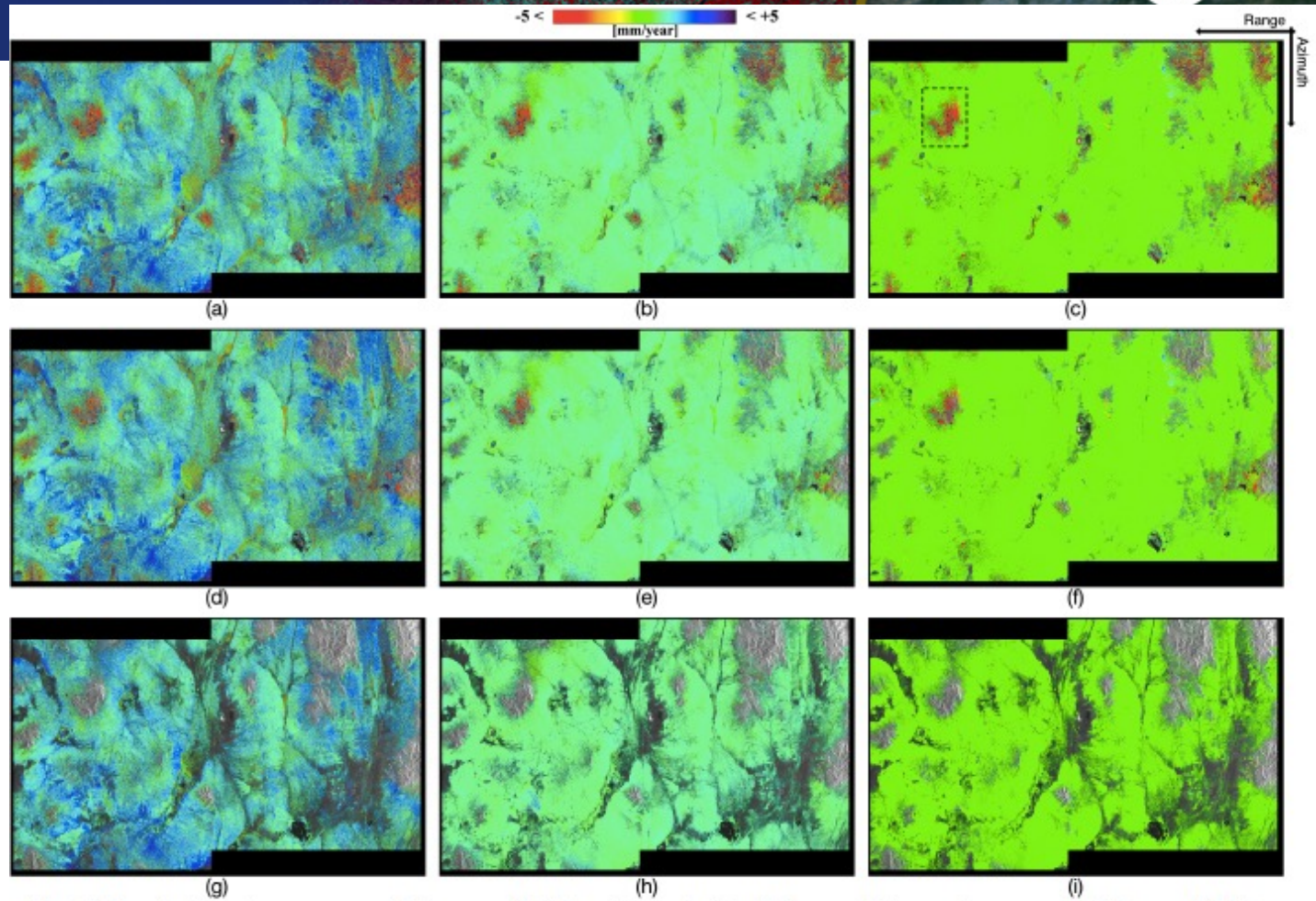


***Fig. 1.*** Nevada test-site area maps of the ground deformation velocity differences between the case at 12 days and 96 days, where only pixels larger than given values of the temporal coherence are depicted. a), d) and g) Ground deformation velocity bias considering the original interferograms. b), e) and h) Ground deformation velocity bias when the time-invariant correction method is applied. c), f) and i) Ground deformation velocity bias when the time-variant correction method is applied. a)-c) Temporal coherence $\geq 0.7$. d)-f) Temporal coherence $\geq 0.9$. g)-i) Temporal coherence $\geq 0.98$.

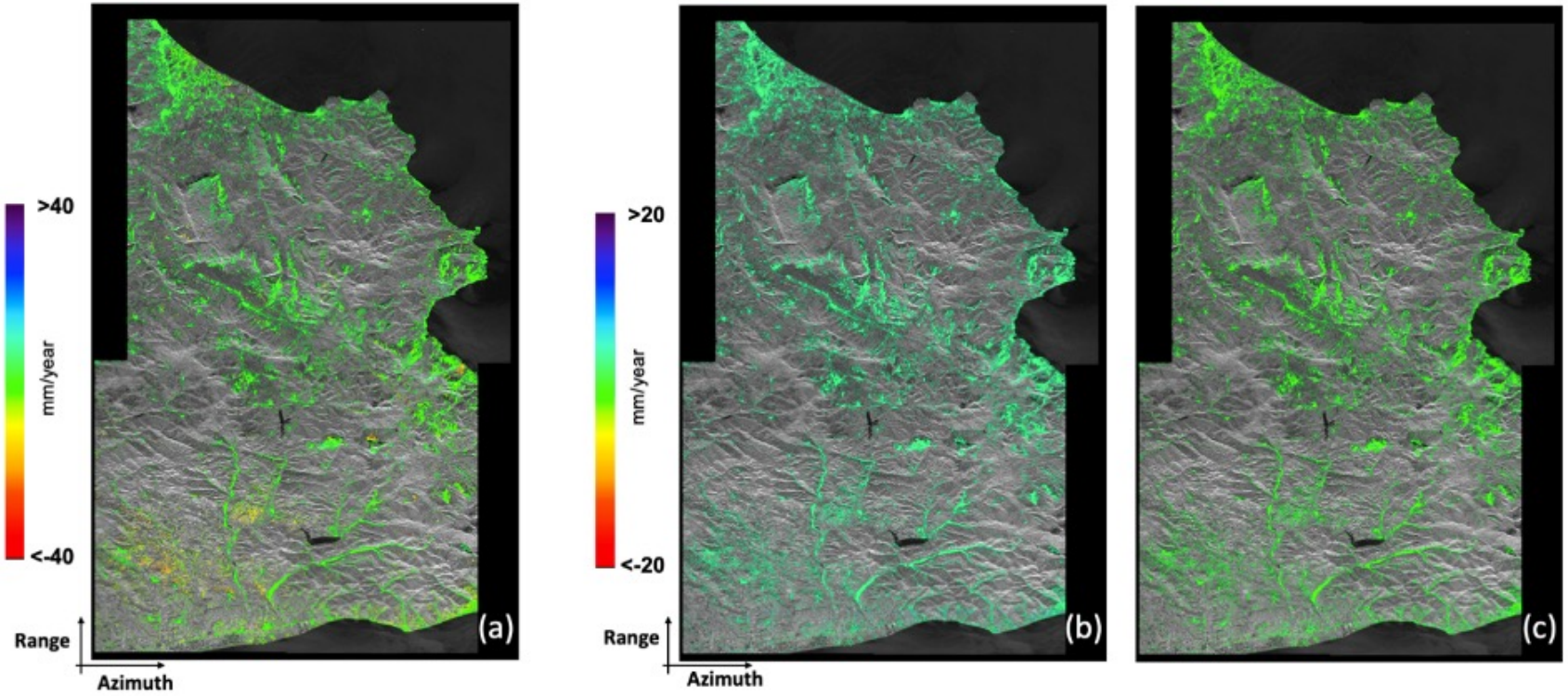


Figure 10. Experiments in Italy: (a) Mean displacement velocity map computed applying the SBAS method to a network of interferograms characterized by a maximum temporal baseline of 148 days. (b) The bias-uncorrected ground deformation velocity differences were mapped using the SB networks at 6 and 148 days. (c) Map of the bias-corrected ground deformation velocity differences between the SB networks at 6 and 148 days. Only pixels characterized by temporal coherence larger than 0.7 are depicted.

# Further Implications: Experiments in Italy

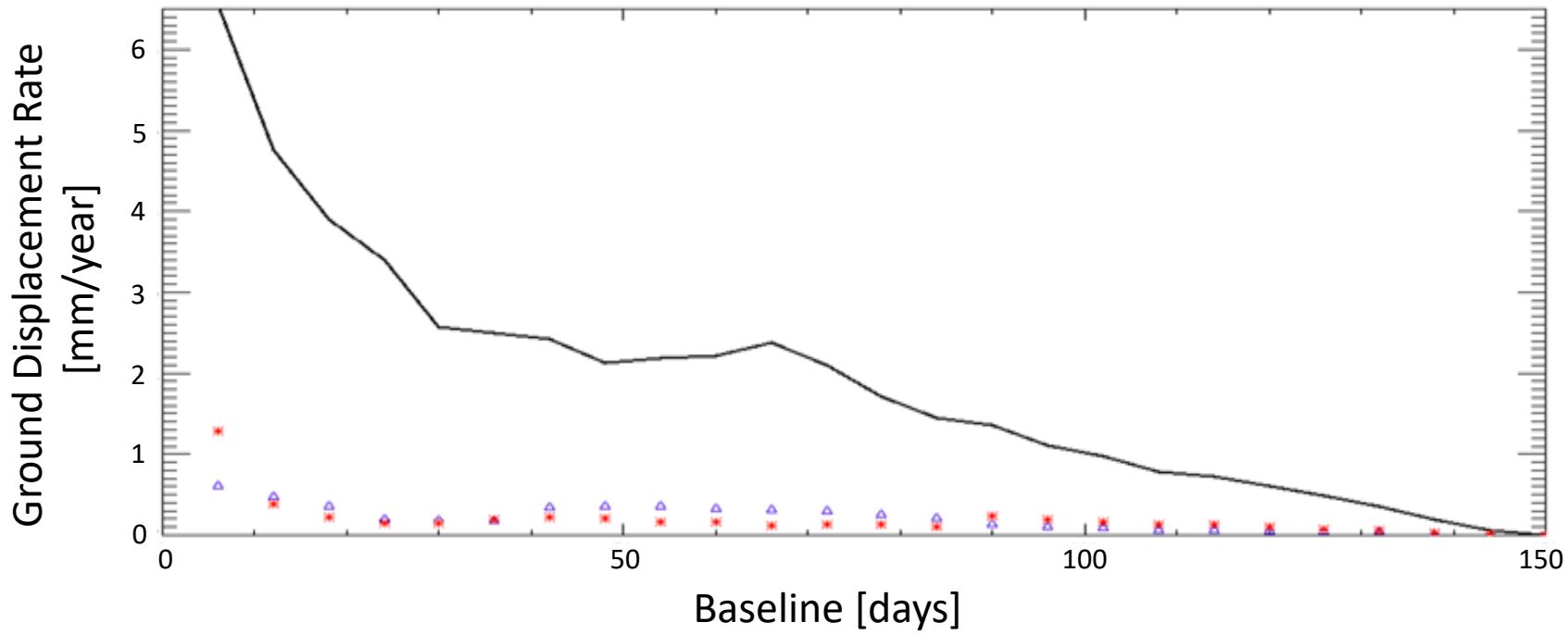

# Ground Subsidence / Urban Sprawl / Change Detection Analyses

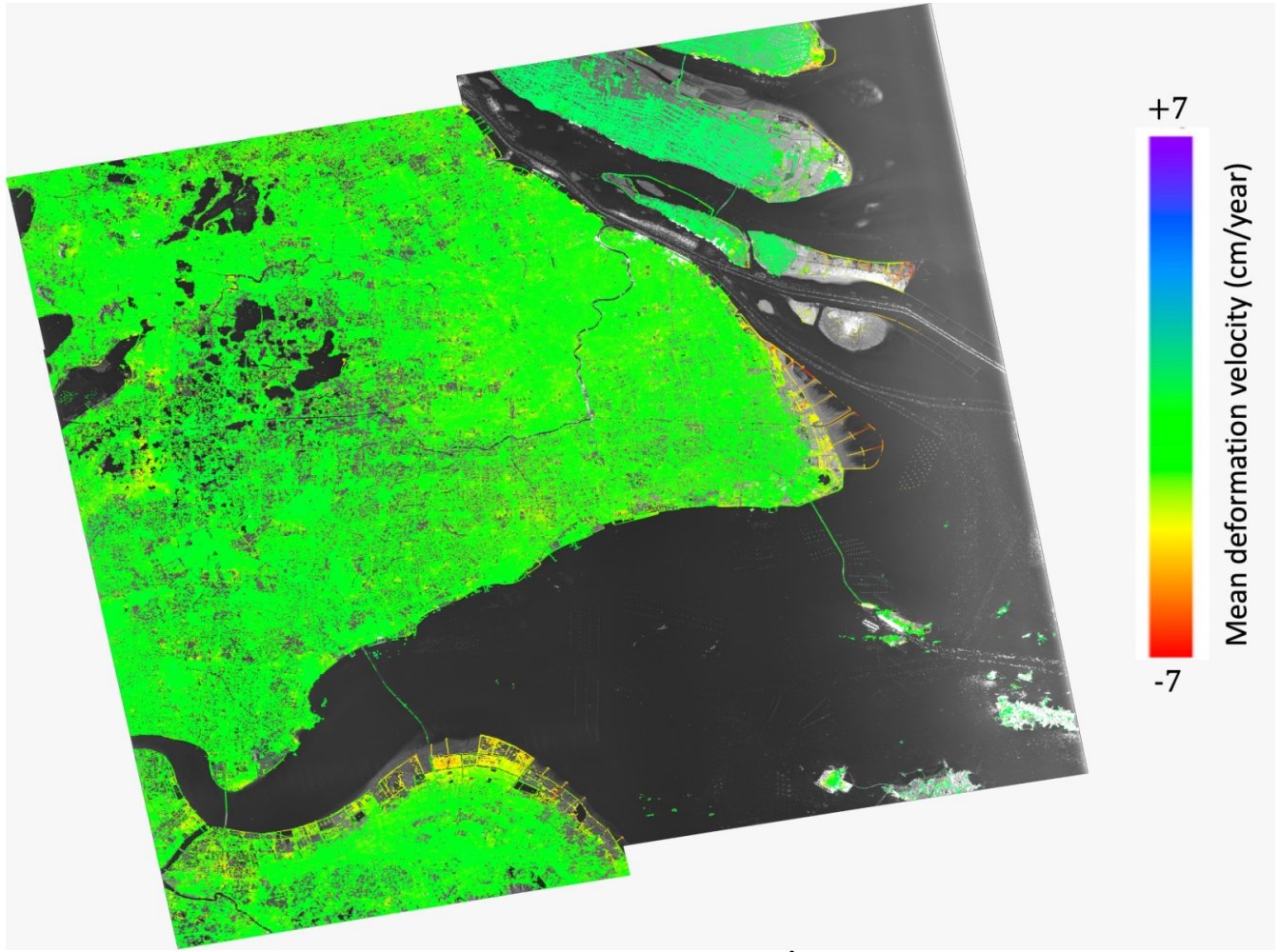


2017 – 2023 Sentinel-1 Data

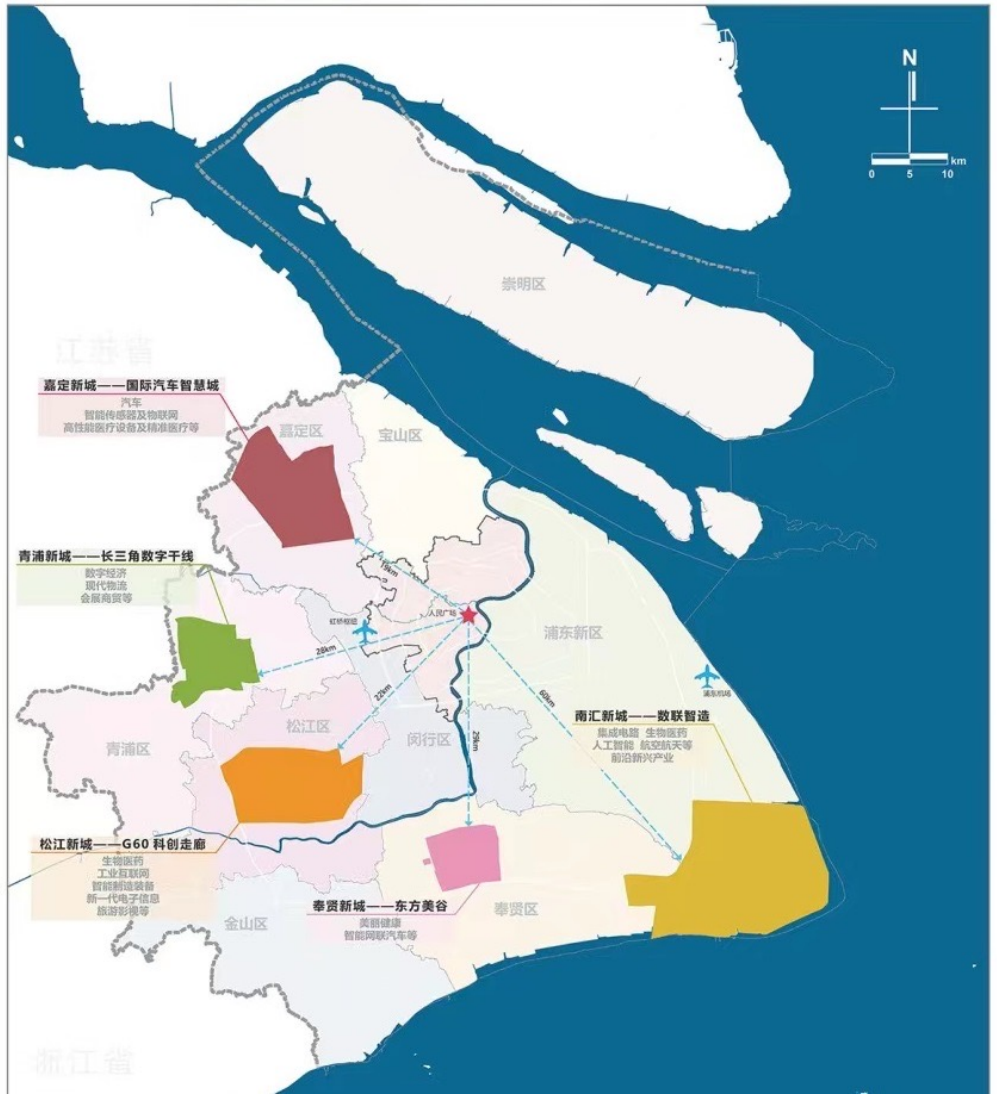

# On-Going Research Activities

- Integration of InSAR and Change Detection methods for the characterization of risk conditions in urban areas
- InSAR-SB Analysis at High Resolution to characterize the damage risk of infrastructures
- Use of AI/ML algorithms to detect and characterize coherent/incoherent changes (damage collapses, new buildings areas)
- Green Restoration and Change Detection

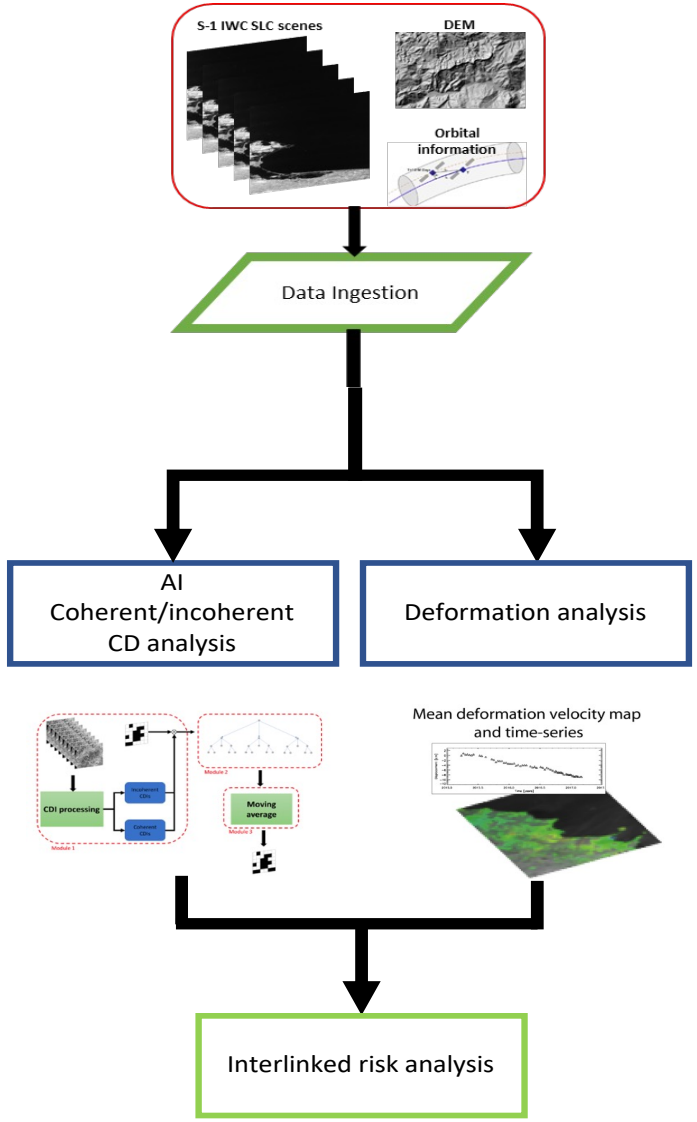


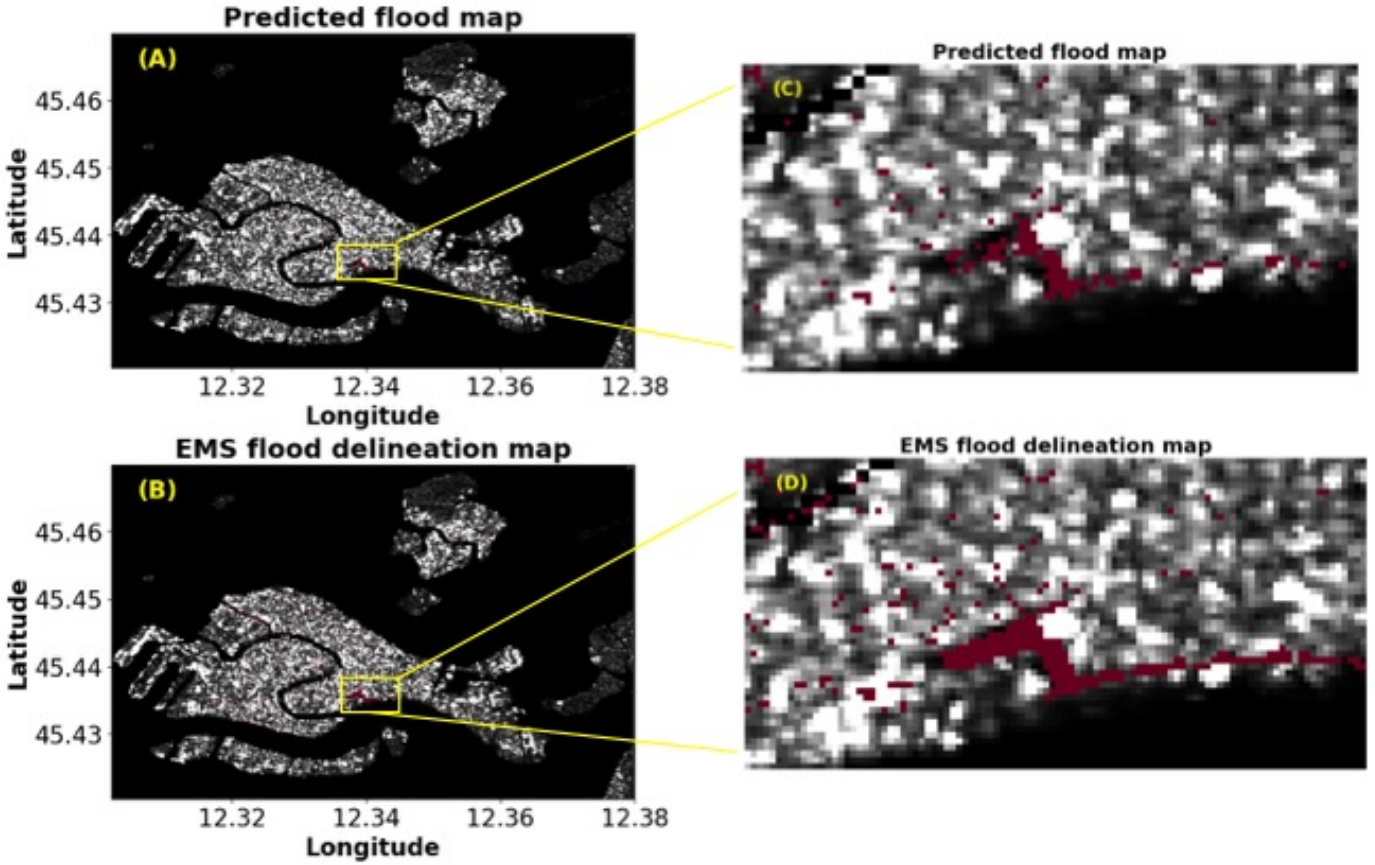


Figure 13. (A) Predicted change masks derived from the proposed methodology and (B) from the Copernicus EMS of Venice city area. Both masks are colored in red and superimposed over SAR amplitude images. Yellow boxes are located in the Piazza San Marco area and zoomed in panels (C) and (D).

# Dragon 5 3rd Year Results Project

**13 SEPTEMBER 2023**

**ID. 58351**

**PROJECT TITLE: GREENISH**

**PRINCIPAL INVESTIGATORS: ANTONIO PEPE, QING ZHAO**

**AUTHORS: ANTONIO PEPE, FABIANA CALÒ, PIETRO MAESTRO, FRANCESCO FALABELLA, VIRGINIA ZAMPARELLI, QING ZHAO**

**PRESENTED BY: QING ZHAO**

# DSPA-Net: A deeply supervised pseudo-siamese attention-guided network for building change detection with intensity and coherence information of SAR images

We propose a deeply supervised pseudo-siamese attention-guided network (DSPA-Net) for BCD, in which convolutional blocks have a good ability in noise reduction owing to the large receptive fields, and the adopted pseudo-siamese structure does well in extracting intensity information and coherence information with the same network branch but different weights.

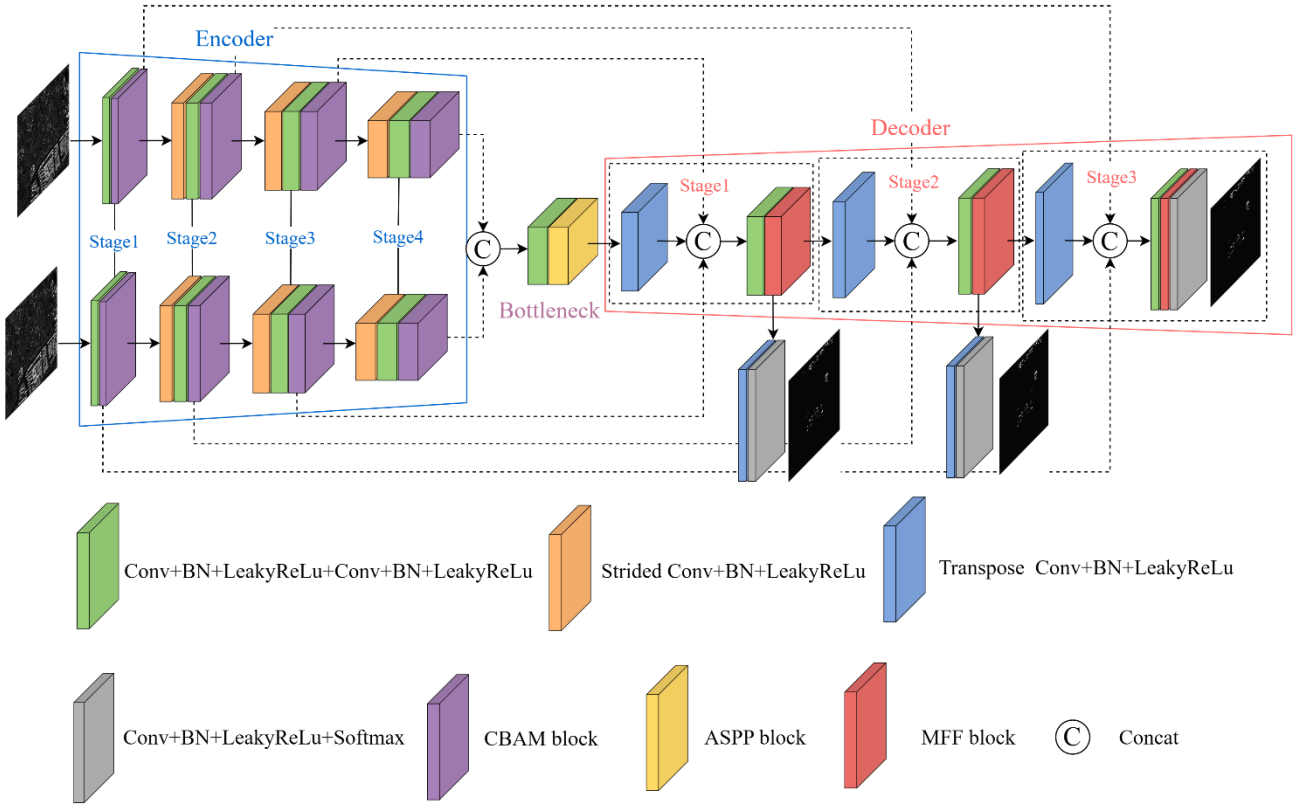


The structure of the DSPA-Net block

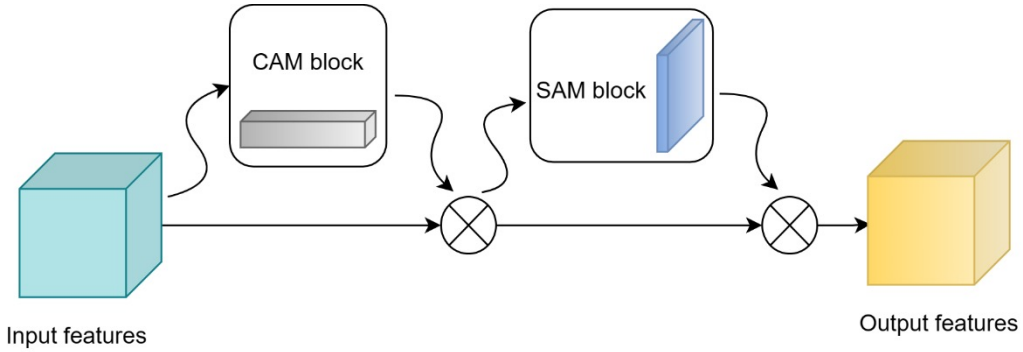


The structure of the CBAM block

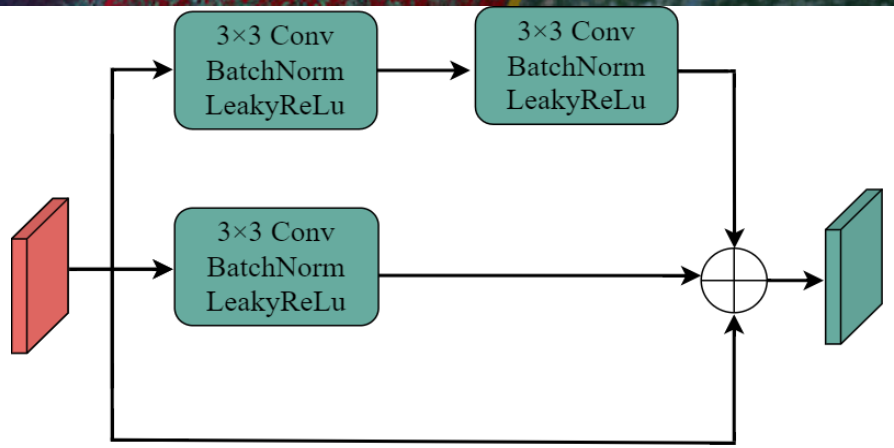


The structure of the MFF block

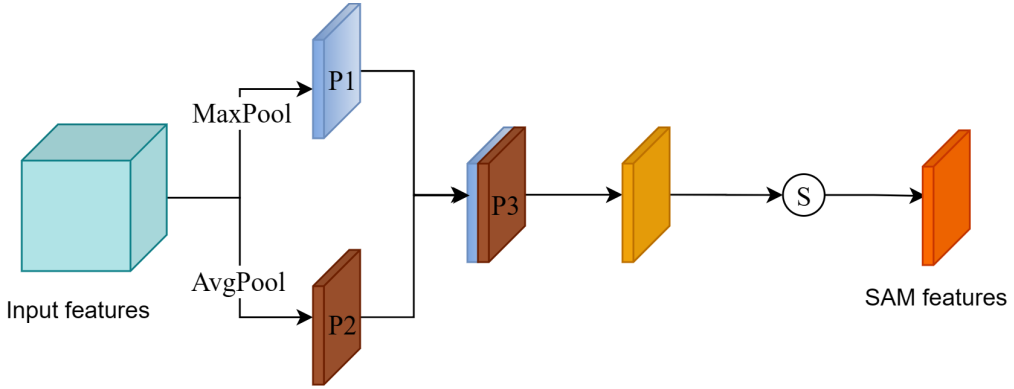


The structure of the SAM block

In the Encoder layer, CBAM block leads to increased attention on building changes. In the Decoder layer, the MFF block is applied to fuse multi-level features and remove the problem of vanishing and exploding gradients caused by the deepening of the network. Besides the supervision on the output layer of the backbone network, DSPA-Net also introduces three deep supervision branches with the same structure.

This study uses high-resolution TerraSAR-X (TSX) images covering Shanghai. Four TSX images are acquired between 16 June 2019 and 10 September 2021. Before training the network, we pre-processed TSX images to get intensity information and coherence information. Intensity information is obtained by pre-processing single-look complex (SLC) images, including radiometric correction, multi-looking processing, and geocoding. Coherence map (CM) is obtained by performing interferometry and computing the coherence values of interferograms.

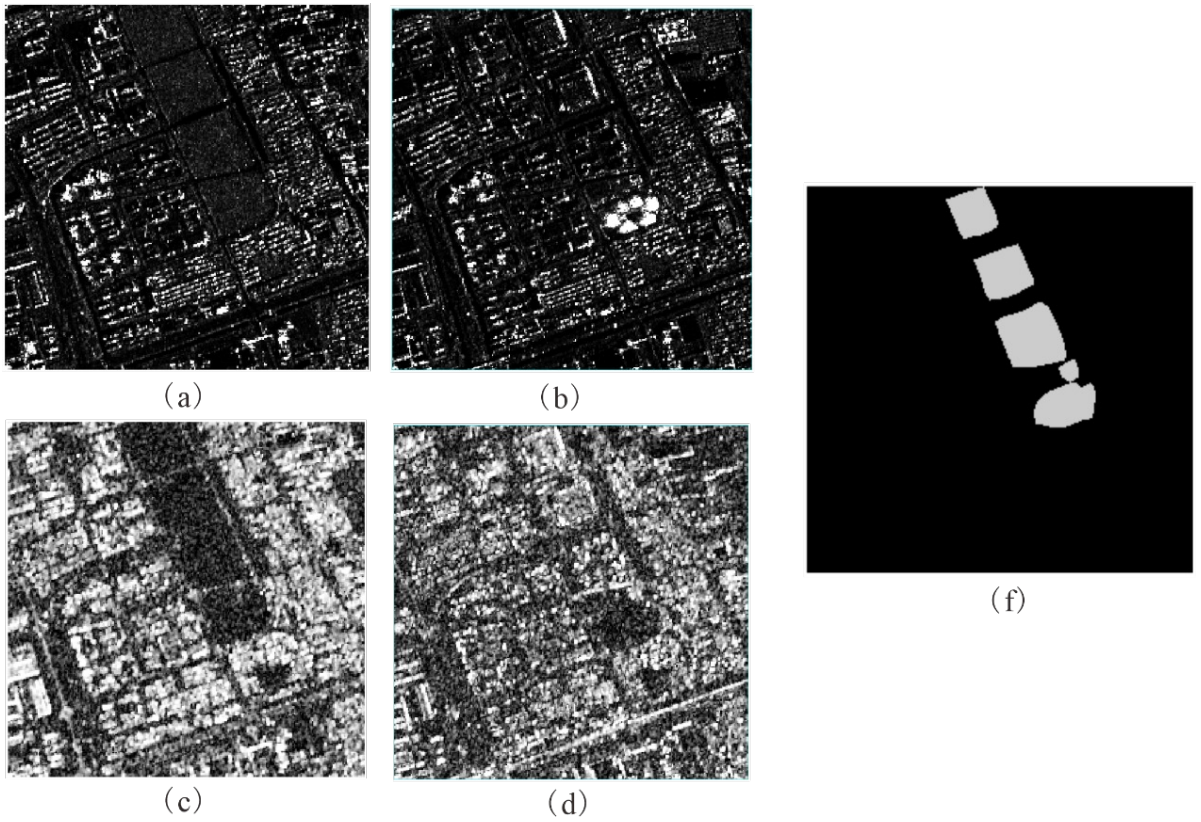


Data set 1. (a)Pre-change SAR intensity image. (b)Post-change SAR intensity image. (c)Pre-change coherence map. (d)Post-change coherence map. (e) Ground-truth image

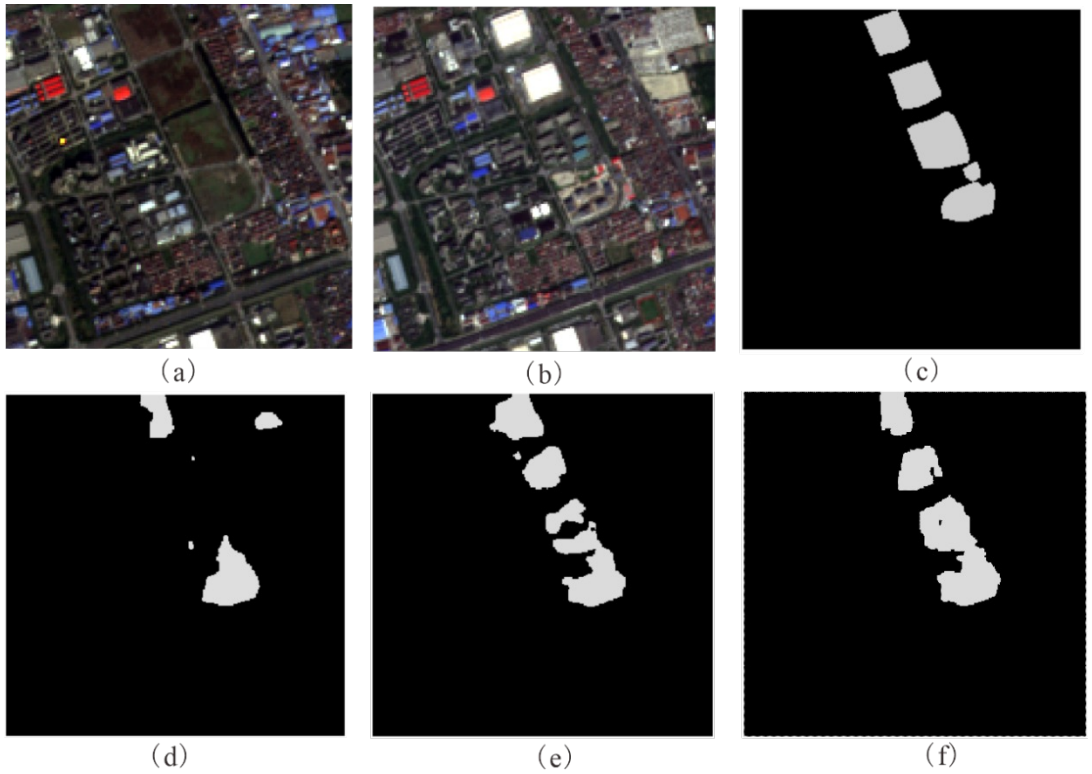


(a) Pre-change optical image. (b) Post-change optical image. (c) Ground-truth image. (d) U-Net, PWR as input data. (e) U-Net, PWR and CM as input data (f) DSPA-Net, PWR and CM as input data

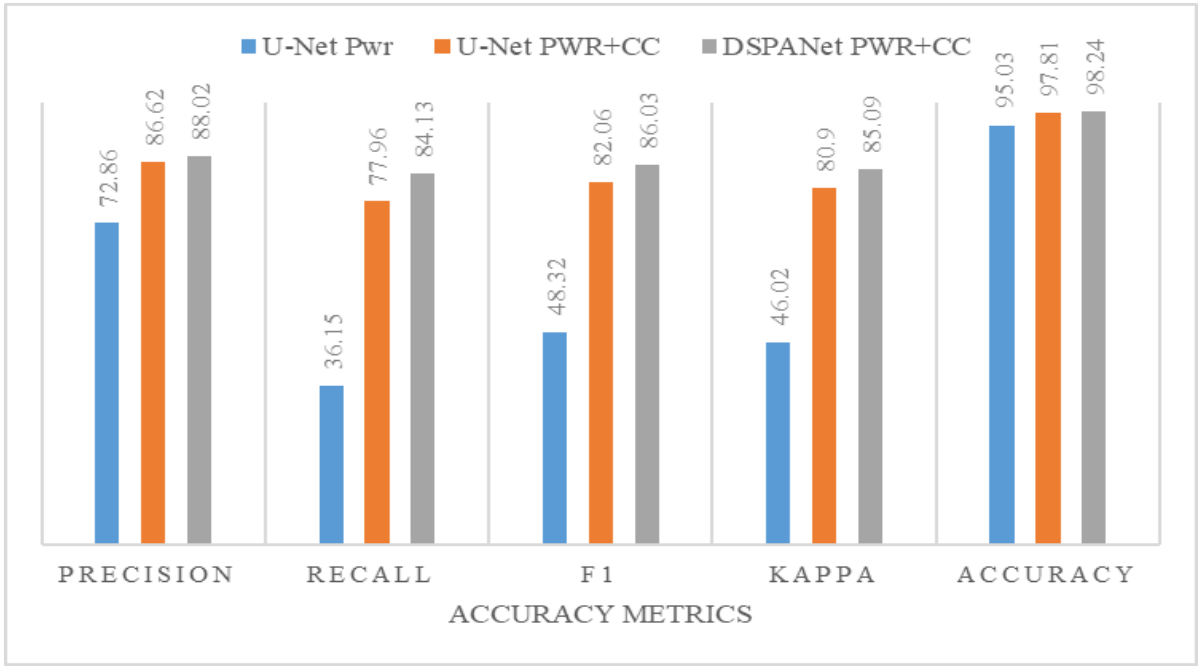


The performance of the DSPA-Net model is superior to the U-Net model, with a gain of 1.4%, 6.17%, 3.97%, 4.19%, and 0.43% for Precision, Recall, F1, Kappa, and Accuracy, respectively.

## Conclusions

The DSPA-Net model aggregates the information of both intensity and coherence information to extract urban building features effectively.

The results show that the method is reliable in urban change detection and performs better than other advanced change detection methods. Its Precision, Recall, F1, Kappa, and Accuracy reach 88.02%, 84.13%, 86.03%, 85.09%, and 98.24, respectively.

# Information extraction and quantifying migration of saltmarsh vegetation in Chongming Dongtan Wetland by integrating multi-source remote sensing data and phenological characteristics during 2017-2022

**EO and other datasets**

- **2 C-band Fine Quad-Pol Rardarsat-2 images from 2021 to 2022**
- **72 C-band Sentinel-1A images from 2017 to 2022**
- **76 multispectral Sentinel-2A images from 2017 to 2022**
- **72 multispectral Landsat8 OLI images from 2017 to 2022**

| Dataset | Description | Acquisition Data |
|---|---|---|
| Dataset1 | Spectral feature + Vegetation index + Textural feature | 2021.9 |
| Dataset2 | Spectral feature + Vegetation index + Textural feature | 2022.2 |
| Dataset3 | Spectral feature + Vegetation index + Textural feature + SAR backscattering feature | 2021.9 |
| Dataset4 | Spectral feature + Vegetation index + Textural feature + SAR backscattering feature | 2022.2 |
| Dataset5 | Spectral feature + Vegetation index + Textural feature | 2021.9 + 2022.2 |
| Dataset6 | Spectral feature+ Vegetation index + Textural feature + SAR backscattering feature | 2021.9 + 2022.2 |

## Methods

- **Gray Level Co-occurrence Matrix algorithm**
- **multi-resolution object-oriented classification algorithm**
- **Random Forest classifier algorithm**
- **Time series analysis algorithm**

Classification accuracy of different datasets based on random forest

| Dataset | OA(%) | Kappa |
|---|---|---|
| Dataset1 | 76.4344 | 0.6981 |
| Dataset2 | 78.0738 | 0.7178 |
| Dataset3 | 78.4836 | 0.7246 |
| Dataset4 | 81.3525 | 0.7601 |
| Dataset5 | 81.8648 | 0.7661 |
| Dataset6 | 90.2980 | 0.8606 |

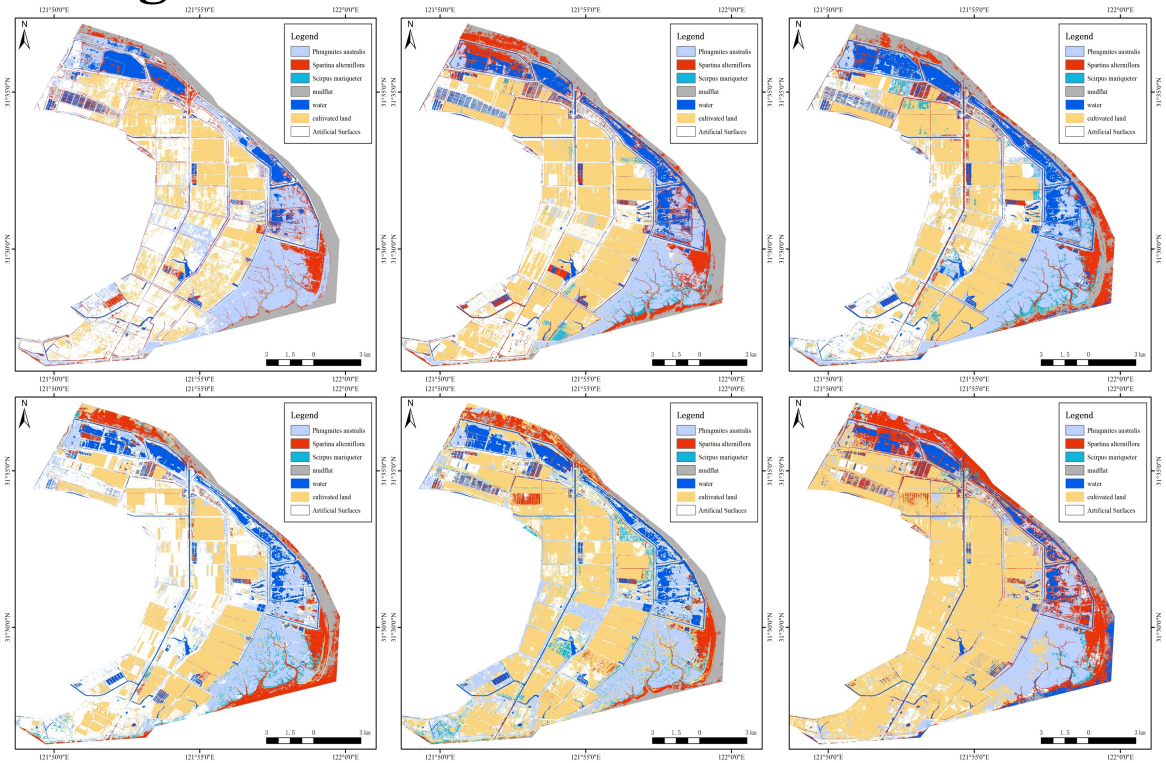


Classification results of study area based on random forest. (a) Datasat1, (b) Dataset2, (c) Dataset3, (d) Dataset4, (e) Dataset5 and (f) Dataset6.

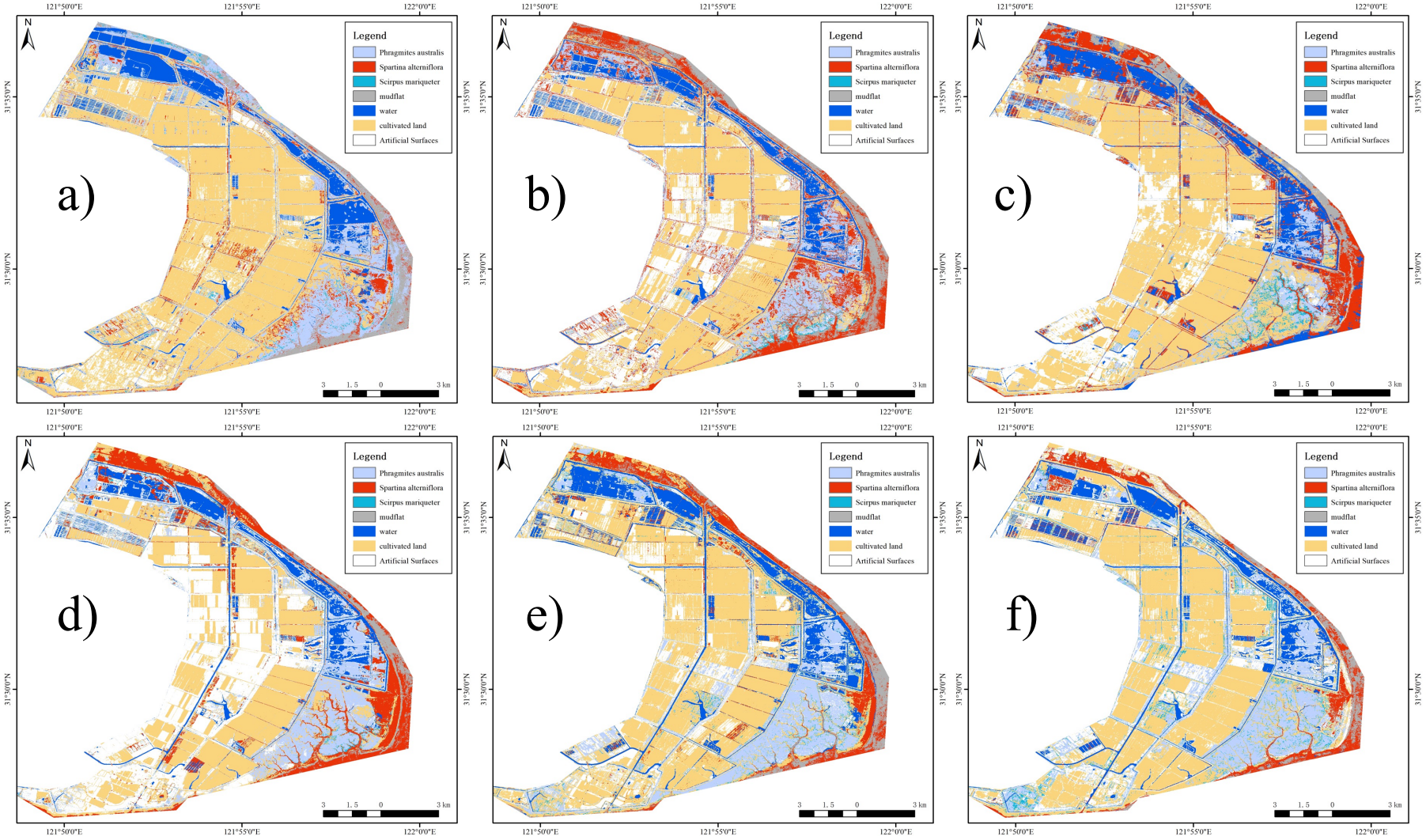


Classification results of study area based on random forest. (a) in 2017, (b) in 2018, (c) in 2019, (d) in 2020, (e) in 2021 and (f) in 2022.

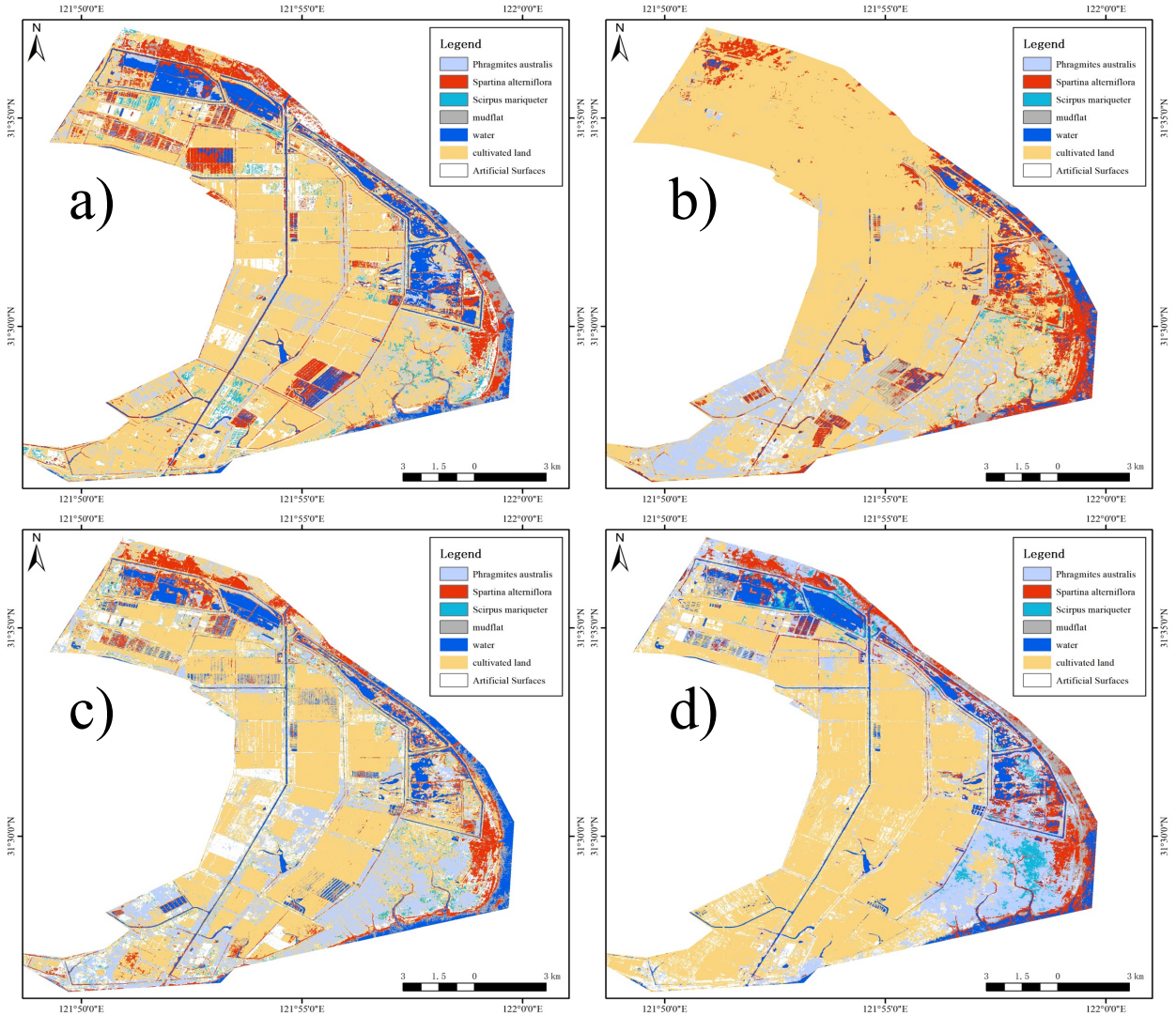


Classification results of study area based on random forest. (a) in 2022 spring, (b) in 2022 summer, (c) in 2022 autumn, and (d) in 2022 winter

# Conclusions

- The study shows that annual maps of saltmarsh vegetation well tracking Spartina saltmarsh's expansion and removal dynamics during 2017-2022 in Chongming Dongtan Wetland.

- The study provides an accurate reference for developing remote sensing inversions in different phenological periods and a method for accurately mapping salt marsh vegetation.

- The resultant annual and multi-year maps of salt marsh vegetation can be used to understand the driving factors of salt marsh vegetation dynamics and assess the impacts of salt marsh vegetation expansion on biodiversity, carbon cycle, and ecosystem services.